THESIS FOR THE DEGREE OF DOCTOR OF PHILOSOPHY

Operational strategies to control the gas composition in dual fluidized bed biomass gasifiers

TERESA BERDUGO VILCHES

Department of Space, Earth and Environment

CHALMERS UNIVERSITY OF TECHNOLOGY

Göteborg, Sweden 2018

Department of Space, Earth and Environment

Division of Energy Technology

Chalmers University of Technology

SE-412 96 Göteboorg

Sweden

Telephone + 46 (0)31-772 1000

Operational strategies to control the gas composition in dual fluidized bed biomass gasifiers

Teresa Berdugo Vilches
Division of Energy Technology
Chalmers University of Technology
SE-412 96 Gothenburg (Sweden)

Abstract

Steam gasification of biomass can increase the share of renewable energy and material resources in the energy sector, transportation and different industries. Prior its application, the raw gas produced in biomass gasifiers needs to be cleaned from impurities. In gasifiers operating at mild temperature, such as fluidized bed steam gasifiers, tar is an impurity of major concern due to the operational problems that it can cause. Tar species can condensate at temperatures as high as 300ºC, causing the clogging of pipes and coolers, deactivating downstream catalysts, and forcing unplanned shut-downs. Thus, it is necessary to control the tar and gas compositions in gasifiers to ensure the technical reliability of the technology.

This work investigates measures to control biomass conversion in dual fluidized bed (DFB) steam gasifiers and, thereby, contribute to the rational operation and design of these types of units. A parametric experimental investigation of the influences of operating conditions on gas and tar compositions is presented. The examined parameters are: fluidization velocity; steam-to-fuel ratio (S/F); circulation rate of the bed material; temperature; and active bed materials. The bed materials tested include silica sand, olivine, bauxite, and feldspar, as well as the oxygen-carrying materials ilmenite and manganese. The work was carried in the Chalmers 2–4-MWth DFB gasifier using woody biomass as the fuel. The gasification technology applied in this work is similar to that of the existing gasifiers at the Güssing, Senden, Oberwart, and GoBiGas plants.

Within the operating window investigated, optimization of the bed material activity was the main tool for controlling tar conversion, which can be improved using additives. The levels of effectiveness of the in-bed catalysts were linked to the destruction of tar precursors. It is proposed that both homogeneous and heterogeneous catalysis of tar reactions occur in systems where alkali is expected in the gas phase. With active bed materials, temperature changes in the range of 700°–830°C were found to affect primarily the composition of the tar, and to a lesser extent, the tar yield. Finally, it is shown that a simple gasifier design with on-bed feeding ensures that at least 50% of the volatiles come in contact with the catalytic bed material when the bed is well-fluidized. Extensive experimental results and their implications for the design and operation of a DFB gasifier are discussed throughout this thesis.

List of publications included in this thesis

This thesis is based on the work contained in the following papers:

I. Teresa Berdugo Vilches, Henrik Thunman. Experimental investigation of volatiles-bed contact in a 2-4 MWth bubbling bed reactor of a dual fluidized bed gasifier. Energy & Fuels, 2015, 29, 6456-6464.

II. Mikael Israelsson, Teresa Berdugo Vilches, Henrik Thunman. Conversion of condensable hydrocarbons in a dual fluidized bed biomass gasifier. Energy & Fuels, 2015, 29, 6465-6575.

III. Teresa Berdugo Vilches, Jelena Maric, Martin Seemann, Henrik Thunman. Comparing active bed materials in a dual fluidized bed biomass gasifier: olivine, bauxite, quartz-sand and ilmenite. Energy Fuels, 2016, 30, 4848-4857.

IV. Nicolas Berguerand, Teresa Berdugo Vilches. Alkali-Feldspar as a Catalyst for biomass gasification in a 2-MW indirect gasifier. Energy & Fuels, 2017, 31, 1583-1592.

V. Teresa Berdugo Vilches, Fredrik Lind, Magnus Rydén, Henrik Thunman. Experience of more than 1000h of operation with oxygen carriers and solid biomass at large scale. Applied Energy, 2017, 190, 1174-1183.

VI. Teresa Berdugo Vilches, Jelena Maric, Daniel Rosenfeld, Pavleta Knutson, Henrik Thunman, Martin Seemann. Bed material as a catalyst for char gasification: the case of ash-coated olivine. Fuel, 2018, 224, 85-93.

VII. Teresa Berdugo Vilches, Martin Seemann, Henrik Thunman Influence of ash-coated olivine on tar formation in steam gasification of biomass. *Submitted for publication.*

Contribution report:

Paper I.   Teresa Berdugo Vilches (TBV) is the principal author, with responsibility for planning of experiments, data evaluation, and writing of the paper.

Paper II.   Mikael Israelsson is the principal author and responsible for the formulation and planning of the paper. TBV contributed with experimental work related to the sand bed experiments, and was responsible for the planning and evaluation of the experiments conducted with ilmenite.

Paper III.   TBV is the principal author and responsible for the formulation of the paper, data gathering, and evaluation. Jelena Maric is responsible for the experimental work with bauxite and olivine, as shares responsibility with TBV for the experiments conducted with olivine and additives. Martin Seemann contributed to the experimental work and with ideas and discussions during the preparation of the manuscript.

Paper IV.   Nicolas Berguerand is the principal author and responsible for planning of the paper and bed material analysis. TBV contributed to the planning and execution of the gasification experiments with feldspar, as well as to the data evaluation and discussions.

Paper V.   TBV is the principal author and responsible for the formulation of the paper, planning and executing the experimental work, as well as the evaluation of the experimental data. Fredrik Lind contributed to the experimental work and editing of the paper. Magnus Rydén contributed with comments on the manuscript.

Paper VI.   TBV is the principal author and responsible for the formulation of the paper and planning of the work. Jelena Maric and Pavleta Knutson contributed with the analyses of the bed material and char particles. Daniel Rosenfeld carried out the char gasification experiments. Martin Seemann contributed with ideas, editing of the paper, and with preparation of the experimental setup.

Paper VII.   TBV is the principal author and responsible for the formulation of the paper, as well as the planning and execution of the experimental work. Martin Seemann contributed to the experimental work and editing of the manuscript.

Professor Henrik Thunman is the principal academic supervisor and has contributed with ideas, discussions, and editing of all the papers included in this thesis.

Related publications not included in this thesis

- Teresa Berdugo Vilches, Erik Sette, Henrik Thunman. Behavior of biomass particles in a large scale (2–4-MWth) bubbling bed reactor. Conference paper, Computational Methods in Multiphase Flow VIII, Valencia, 2015.

- Erik Sette, Teresa Berdugo Vilches, David Pallarès, Filip Johnsson. Measuring fuel mixing under industrial fluidized-bed conditions – A camera-probe based fuel tracking system. Applied Energy, 2015, 163, 304−312

- Nicolas Berguerand, Jelena Marinkovic, Teresa Berdugo Vilches, Henrik Thunman. Use of alkali-feldspar as bed material for upgrading a biomass-derived producer gas from a gasifier. Chemical Engineering Journal, 2016, 295, 80-91.

- Teresa Berdugo Vilches, Henrik Thunman. Impact of oxygen transport on char conversion in dual fluidized bed systems. Conference paper, Nordic Flame Days, Copenhagen, 2015.

- Sébastien Pissot, Teresa Berdugo Vilches, Martin Seemann. Influence of the S-K interactions on a dual fluidized bed system. Conference paper, Nordic Flame Days, Stockholm, 2017.

- Sébastien Pissot, Teresa Berdugo Vilches, Henrik Thunman, Martin Seemann. Effect of ash circulation on the performance of a dual fluidized bed gasification system. Biomass and Bioenergy, 2018, 115, 45-55.

- Henrik Thunman, Martin Seemann, Teresa Berdugo Vilches, Jelena Maric, David Pallares, Henrik Ström, Göran Berndes, Pavleta Knutsson, Anton Larsson, Claes Breitholtz & Olga Santos. Advanced biofuel production via gasification - Lessons learned from 200 man-years of research activity with Chalmers' research gasifier and the GoBiGas demonstration plant. Energy Science Engineering, 2018, 6, 1, 6-34.

Acknowledgments

Behind the scenes of this thesis, there are a lot of wonderful people who have contributed, in a way or another, to the completion of this work. I would like to start by expressing my most sincere gratitude to my main academic supervisor Henrik Thunman for the opportunity to pursue a PhD, for your guidance, enthusiasm, and for all the opportunities you have given to me to develop my skills as researcher. Thanks to Martin Seemann and Fredrik Lind for being always eager to discuss, for your support during experiments, and your inspiring attitude towards research. To Nicolas Berguerand, for first introducing me to the experimental work at Chalmers.

I am grateful to the *gasification gang* that welcomed me when I started: Jelena Maric, Mikael Israelsson, Anton Larsson, Alberto Alamia, Erik Sette, Huong Nguyen, and Louise Lundberg for making me feel part of the team from the very first day. Special thanks to Jelena, for your exceptional help in the long (and usually fun) days of experiments, for the enriching discussions about research and for being a friend. Thanks to Mikael, for sharing with me all the mysteries of SPA and *Inferno,* which have been so useful in my work. To Erik and Alberto, thanks for a long-lasting friendship. To the more recent members of the team, Sébastien and Isabel, thanks for continuing the tradition of a nice and collaborative research group. To the rest of colleagues at the Energy Technology Division, thanks for creating a friendly and stimulating working environment.

Since I started my PhD, I have spent the cold winters in one of the warmest spots in Sweden: Kraftcentralen (KC), a place full of extremely competent and kind people. To the research engineers Jessica Bohwalli, Johannes Öhlin and Rustan Hvitt, thanks for your irreplaceable support with your technical expertise. Thanks to the operating staff (former and current) at Akademiska Hus: Rikard, Petrus, Robban and Mikael for the operation of the boiler. To all of you, thanks for your patience with my habit of taking *one more point*.

Por último, a mis padres, Rafael y María Jesús, y a mi hermana, Ana, por vuestro apoyo incondicional a pesar de la distancia que nos separa. À Alex, merci d'être toujour là pour moi.

Teresa Berdugo Vilches, Göteborg 2018

To my father

Table of Contents

1 - Introduction

Current concerns regarding climate change, depletion of resources, and waste accumulation, call for technical solutions that will limit the global temperature rise and, at the same time, enable a shift from a linear to a circular economy. Accordingly, the European Union is promoting the transition from a fossil fuel-based to a carbon-free energy sector. By Year 2030, Europe should reach 27% (at minimum) share of renewables in the final energy consumption [1], and a 40% (at minimum) cut in greenhouse gas (GHG) emissions [2]. Gasification of biomass offers the possibility to reduce GHG emissions and increase the shares of renewable resources in different sectors. As summarized in Figure 1, gasification-based processes can be designed for the production of heat, electricity, and syngas, which can be further processed into H_2, or used for synthesis of biofuels and chemicals. Biomass-derived products can replace their existing fossil-based counterparts, such as gas and oil-based fuels for the transportation sector, as well as H_2 and syngas, which are currently produced from steam reforming of natural gas and naphtha.
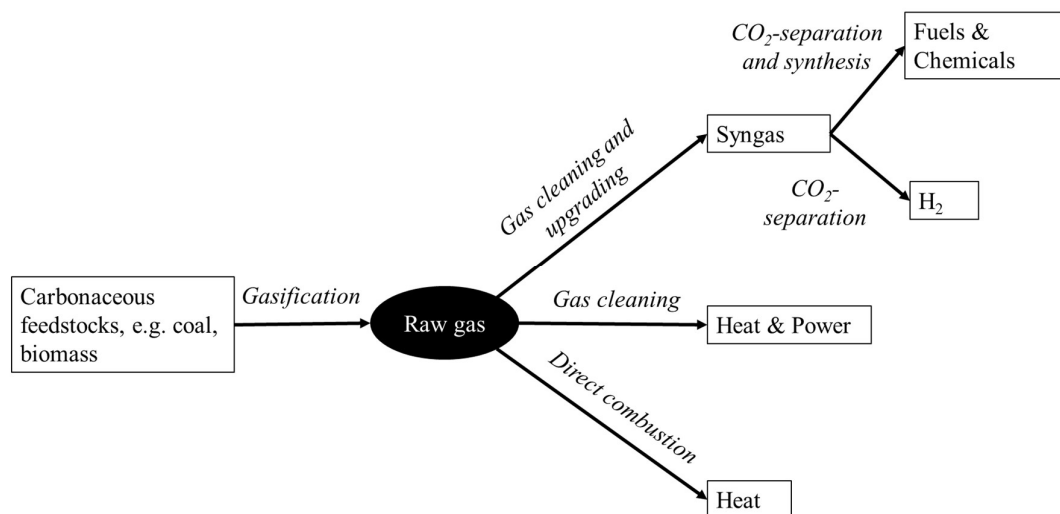
Figure 1. Potential final products of a gasification-based process.

Gasification is a thermochemical process to convert any carbonaceous feedstock, e.g., coal and wood, into an energy-rich gas (i.e., raw gas). The raw gas generated by the gasification of biomass is typically rich in H_2, CO, and CO_2, with smaller fractions of CH_4 and other hydrocarbons. The exact composition of the gas reflects the operating conditions applied in the gasifier and the fuel applied. In contrast to coal gasification, biomass fuels have higher contents of volatiles, which are released rapidly in the gasifier (30–40 s for wood pellets [3]) and contain 60%–68% of the carbon content of the parent fuel. This implies that the volatiles released during

the primary pyrolysis stage are major contributors to the production of gas, as shown in Figure 2. The contribution of char to the production of gas is moderate due to its comparatively smaller share, combined with the expected incomplete conversion given the limited residence times (i.e., minutes) of industrial gasifiers. For instance, full steam gasification of a wood char pellet would require a residence time >30 minutes at 840°C [4].
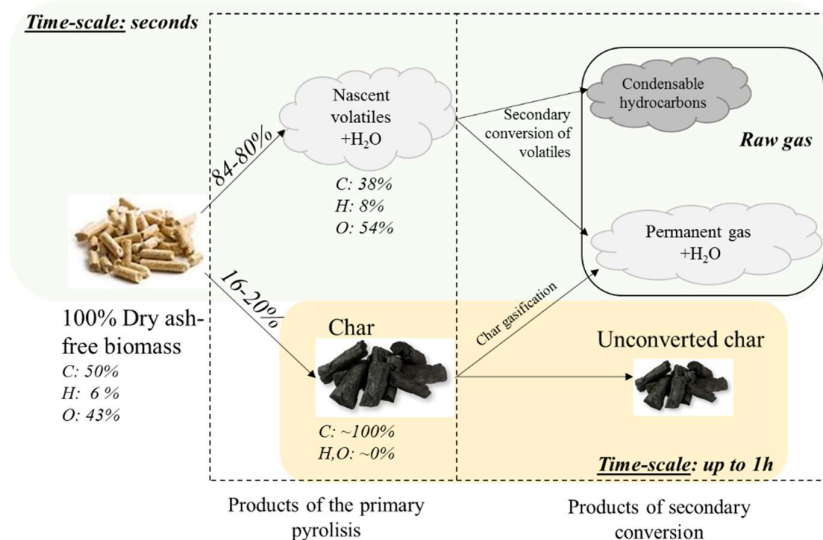
Figure 2. Products of the primary pyrolysis and secondary conversion reactions during thermochemical conversion of biomass in a steam environment. The percentage values correspond to % mass.

Secondary conversion of the biomass-derived volatiles involves cracking and steam reforming reactions, which determine the final composition of the produced raw gas, and more importantly, the final concentrations of tar species. Tar, which is formed as a by-product of the cracking reactions, is considered the major technical challenge for the biomass steam gasification technology at mild temperatures [5]. Therefore, the tar concentration should be controlled to ensure the efficacy of the downstream processes. For instance, tar condenses at temperatures in the range of 300°–400°C, leading to the clogging of pipes and coolers [5], and resulting in unplanned shut-downs that restrict the availability of the process. Additional restrictions linked to the concentration of tar depend on the final application of the product gas; some of the reported upper limits are listed in Table 1.

Table 1. Reported tar limits for various applications. Compiled from [5, 6]

Application	Upper concentration limit for tar
Direct combustion	No limit specified
Gas turbine	<5 mg/Nm^3
IC engines	<100 mg/Nm^3
Fisher-Tropsch synthesis	<1 ppmv
Methanol synthesis over CuO/ZnO	<0.1 mg/Nm^3
Pipeline transport (compressors)	50–500 mg/Nm^3

Measures to control the tar concentration can be considered at the gasifier stage (primary measures) and/or downstream of the gasifier (secondary measures) [7]. Primary measures, which are the focus of this work, are attractive because they can simplify the process layout [7, 8]. Primary measures involve the appropriate choice of operating conditions, including the process temperature, steam-to-fuel ratio, and types of catalysts used. While all sets of operating conditions influence the raw gas composition to some extent, the relative effectiveness of various primary measures has seldom been examined. Nevertheless, the application of catalysts is a commonly used measure in commercial gasifiers, so it receives special attention in this thesis. The concept of gasification with in-bed catalysis has been demonstrated in, for example, the GoBiGas plant in Gothenburg [9] and the Güssing gasifier [10].
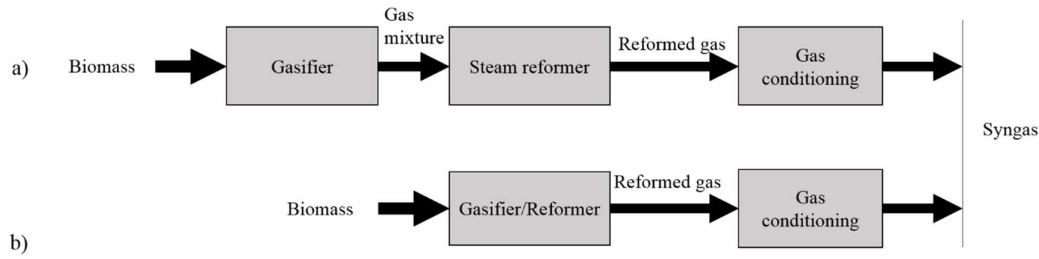
Figure 3. Simplified schemes for the catalytic production of syngas from biomass. a) Devolatilization followed by downstream reforming of volatiles. b) In situ devolatilization and steam reforming.

In-bed catalysis combines the gasifier and the catalytic conversion of volatiles in the same reactor volume, as depicted in Figure 3. Gasification with integrated catalytic conversion of volatiles can be implemented in an indirect gasifier (IG), where the sole oxidizing agent is steam. Typically, the reactor used for indirect gasification is a dual fluidized bed (DFB), which is used in this work and described below.

1.1 Conversion of volatiles in a steam environment

In a steam gasifier, the secondary conversion of volatiles involves the superimposition of cracking and reforming reactions. Thus, the hydrocarbons are cracked into lower-molecular-weight species (R2) and/or they are steam-reformed into carbon oxides and hydrogen (R1), as shown schematically in Figure 4. The extents of cracking and steam reforming in a steam gasifier are influenced by the composition of the fuel [11], the operating conditions [12, 13], and the catalyst applied [14]. The typical operating conditions for a steam gasifier and its fossil fuel counterpart processes (i.e., steam cracking and steam reforming) are summarized in Table 3.

Table 2. Important reactions that occur in steam gasifiers operated at atmospheric pressure.

$C_xH_y + xH_2O \rightarrow xCO + (y + 2x)/2\ H_2$	(R1) Steam reforming of hydrocarbons
$C_xH_y \rightarrow C + C_kH_z + H_2$	(R2) Thermal cracking
$CO + H_2O \leftrightarrow CO_2 + H_2$	(R3) Water-Gas Shift (WGS) equilibrium
$C + H_2O \rightarrow CO + H_2$	(R4) Steam gasification of char
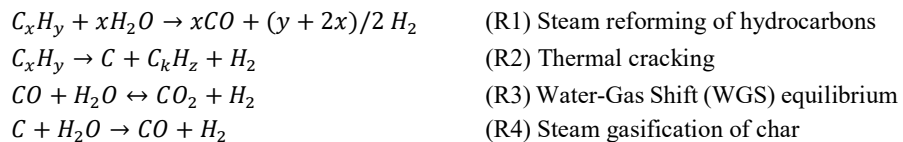
Figure 4. Simplified scale of the molecular complexity of hydrocarbon products and the corresponding pathway to simpler molecules.

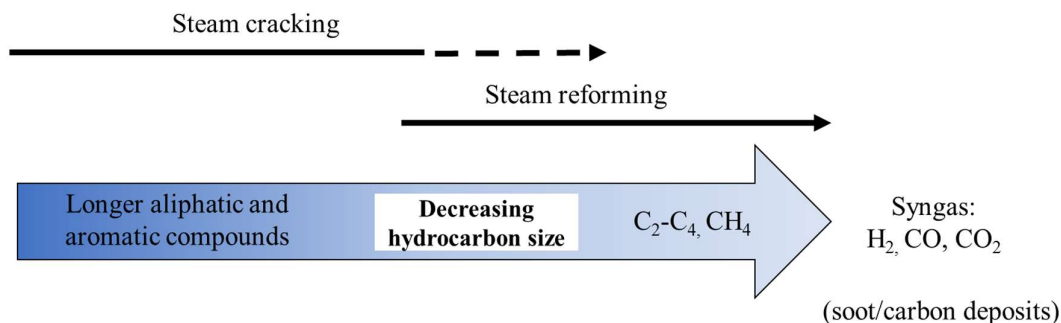The chemistry of steam cracking is relevant to the initial cracking of nascent volatiles into permanent gases in the gasifier, and to the side-reactions that drive tar formation. Thermal cracking follows a free radical-based mechanism and it proceeds rapidly at the temperatures relevant to gasification [15]. To avoid excessive cracking in industrial crackers, the reactions are quenched after a period not exceeding 0.5 s [16]. In steam gasifiers, cracking proceeds for several seconds, which results in the production of mainly short and stable hydrocarbon molecules, e.g., CH_4 and C_2H_4. Higher residence times and/or temperatures yield lower-molecular-weight hydrocarbons, although undesired side-reactions are generated. Common side-reactions in steam cracking include carbon formation and the polymerization of hydrocarbons through the recombination of free radicals [16], which in biomass gasification leads to tar formation via polyaromatic growth [17].

Table 3. Comparison of typical operating conditions for industrial steam crackers, steam reformers, and steam gasifiers.

	Steam cracking	**Steam reforming**	**Steam gasification**
Feedstock	Naphtha	CH_4, naphtha	Solid carbonaceous feedstocks, e.g., woody biomass
Product	Hydrocarbons lighter than the feed	Syngas (usually at equilibrium)	Syngas and minor fractions of hydrocarbons
Temperature	750°–875°C	600°–900°C	800°–900°C
Pressure	Approx. 2 bar	Approx. 20 bar	Approx. atm
Catalyst	Non-catalytic	Ni-based	Optional
S/F (kg steam/kg feed)	0.2–1.0	3.0–4.0	0.5–1.0
Role of steam	Inert	Reactant	Reactant
Residence time	0.1–0.5 s	<1 s	>3 s

Steam reforming (R1) is slower than cracking at the temperatures relevant to gasification, and in practice, this reaction is assisted by a catalyst, e.g., Ni. In commercial steam reformers, the product gas reaches equilibrium by the time it exits the reactor [18]. In contrast, in steam gasifiers, equilibrium is not reached despite the longer residence time and the presence of catalysts, e.g., non-equilibrium levels of CH_4 and C_2H_4 are present in the gas. The only relevant equilibrium in gasifiers is the Water-Gas Shift (R3), and equilibrium is usually not attained [19]. An important side-reaction in steam reforming is the formation of carbon deposits, which

follows the dissociation of the hydrocarbons on the surface of the catalyst. This is minimized by providing excess steam to favor the steam gasification reaction [20]. In atmospheric steam gasification, the excess steam concentration is usually sufficient to render carbon deposition thermodynamically unfavorable, even though carbon deposition on catalyst particles can occur [21-23].

1.2   Dual fluidized bed (DFB) gasifiers

A DFB gasifier functions simultaneously as a chemical reactor and an energy converter. The net reaction in the gasifier/reformer is endothermic and the heat required is supplied externally by combustion. This configuration separates the combustion reactions from the processes of pyrolysis and secondary volatile conversion, and it avoids mixing the product gas with air or flue gases. The DFB gasifier consists of two interconnected fluidized bed reactors (Figure 5a), a combustor and a gasifier/reformer, respectively. A hot bed material, or catalyst, circulates between the reactors, thereby transferring heat from the combustor to the gasifier. The reactors are separated by loop seals (LS), which enable the flow of bed material while preventing any mixing of the two gas environments [24].

The physical separation of the chemical reactor and the heat source (combustion) is also applied in commercial steam reformers [18] and steam crackers [16]. In steam reformers/crackers, reactor tubes are hosted inside a furnace, as illustrated in Figure 5b. The carbonaceous feedstock (e.g., natural gas, naphtha) is reformed/cracked inside the tubes, while the combustion takes place outside the tubes. The heat that is released in the furnace is transferred to the reformer/cracker tubes via radiation and convection to the tube walls [25]. An advantage that the DFB concept has over tubular reactors is that carbon deposits on the surface of the catalytic bed are removed continuously in the combustor, as occurs in commercial Fluid Catalytic Crackers.
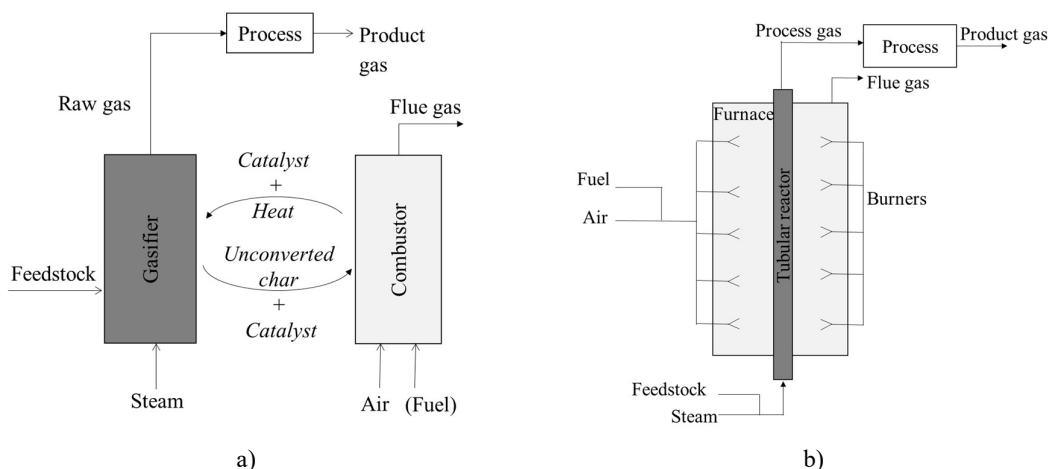

Figure 5. Schematics of a dual fluidized bed steam gasifier and an example of a tube from a steam reforming/cracking tubular reactor

The use of solid biomass in a catalytic process is technically challenging because it involves: (1) a fuel with high content of volatiles; and (2) impurities, such as sulfur, tar and alkali species.

5

The large fraction of volatiles is problematic in terms of the mixing of the catalyst and volatiles [26], while the impurities poison commercial steam-reforming catalysts [27, 28] and can have a deleterious effect on the tar reduction ability. Furthermore, it is unclear as to whether optimized selection of operating conditions (e.g., temperature, S/F) is sufficient or necessary to ensure the long-term availability of the process and the controlled production of gas and tar species. Therefore, a good understanding of the relative influences of design and operating choices for the production of tar is essential towards designing a reliable biomass gasification process.

1.3 Aim and scope

The aim of this thesis is to identify effective operational strategies for controlling the degree of conversion of woody biomass in fluidized bed steam gasification, i.e., those parameters that influence the conversion of the biomass into gas species. The most important output of this thesis is a set of measures to control fuel conversion in DFB units, thereby contributing to the rational design and reliable operation of DFB gasifiers.

Relevant operating variables for DFB gasifiers are summarized in Figure 7, where the asterisks indicate those variables that have been investigated in the course of this work. The operating variables can alter the effective time of reaction (τ) by changing the mixing patterns, and/or they alter the reaction rate (r).
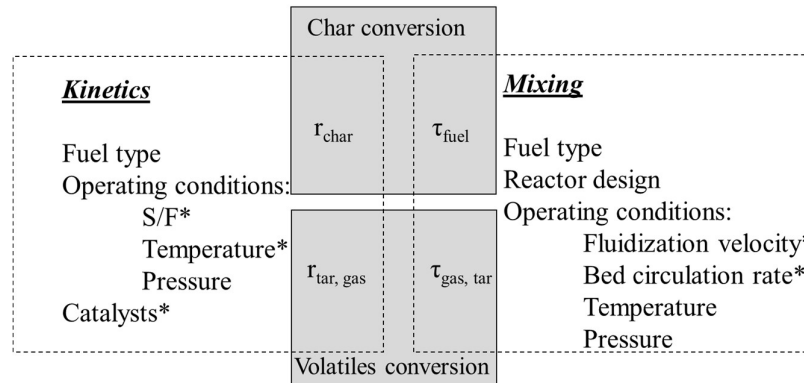
Figure 6. Operating conditions that influence fuel conversion by altering the fluid dynamics and the chemistry in the DFB gasifier. *Parameters investigated in this thesis. The variable (τ) refers to the effective time for the reaction and (r) refers to the reaction rate. S/F refers to the steam-to-fuel ratio.

1.4 Outline of the thesis

This thesis comprises the main findings from a series of seven scientific papers. This research work has been both explorative and applied, with the driver being to understand the interrelationship between operating conditions and the product distributions in DFB gasifiers. Most of the thesis is concerned with experimental research to explore the influences of different operating conditions on the raw gas composition. The development of the research work and its relation to the research papers are schematized in Figure 7.

6
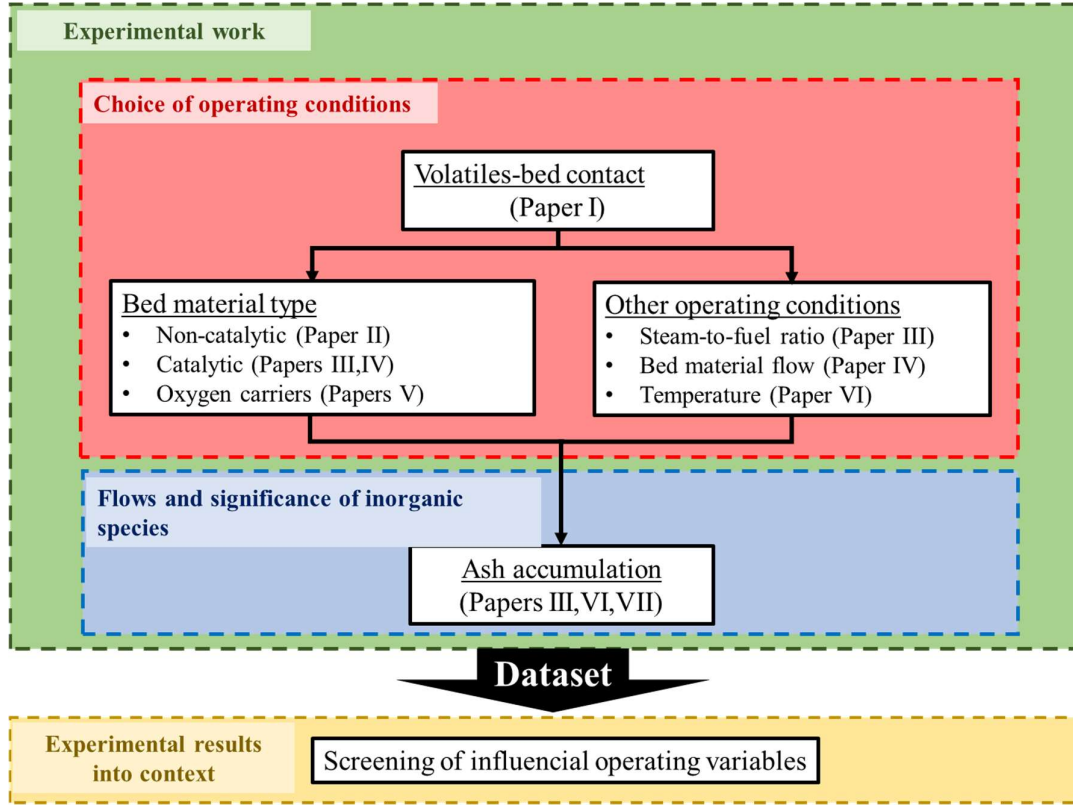
Figure 7. Overview of the research paths and the relationships to the papers included in this thesis. The green area encompasses the experimental work, and the yellow area represents the analyses of the generated dataset.

The initial goal of this work was to acquire an understanding of the extent of the mixing that occurs between volatiles and bed material in the fluidized bed gasifier. The extent of this mixing has been much debated in the research community, with significant consequences for the design of fuel feeding systems for commercial gasifiers. The contribution to this discussion is covered in **Paper I**.

The influences of operational conditions on the fuel conversion were then mapped. The explored variables were: bed material type; temperature; S/F; and circulation rate of the bed material. The reference point to interpret the experimental data is **Paper II**, which covers the mapping of operational conditions with a bed of silica sand, which is generally considered as reference material [14] due to its low catalytic activity. Active materials (e.g., oxygen carriers and catalytic bed materials) in combination with various operational conditions are described in **Papers III–VI**.

An early finding in the work of this thesis was that ash accumulation in the bed material has a strong influence on the outcome of the gasifier, as reported in **Paper III**. Therefore, dedicated experiments were carried out to elucidate the relationship between ash accumulation and fuel conversion, with the focus placed on char in **Paper VI** and on tar in **Paper VII**.

In concluding this research, an effort is made to elucidate the relative influences of the different operating variables on tar formation in gasifiers. For this purpose, the database generated in the course of the work for this thesis is visualized in relation to selected gas quality indicators. The aim here is to place the operating strategies into context, and to distinguish between priority measures for controlling tar formation and those measures that yield only a marginal improvement in tar reduction.

The thesis is structured as follows: the fundamentals of the relationship between operating conditions and product distribution are described in Chapter 2, while the ash flows in DFB systems and their relevance to fuel conversion are described in Chapter 3. Chapter 4 outlines the experimental setup, the materials used and the evaluations of the experiments. A selection of important results is summarized and discussed in Chapter 5. Concluding remarks and recommendations for further research in the field of gasification are provided in Chapters 6 and 7, respectively.

2 - Choice of operating conditions for DFB Gasifiers

The choice of operating conditions for a commercial gasifier is restricted to a relatively narrow operating window, which ensures trouble-free operation, while providing the highest possible yield of the desired species. As shown in Table 4, a state-of-the-art DFB gasifier operates with olivine as the bed material, S/F of 0.5–1.0 kg/kg daf fuel, and a gasifier temperature in the range of 830°–870°C. In contrast, for the Chalmers gasifier, the flexibility of operation is greater, as the reactor is built for research purposes and there is no imposition of downstream equipment requirements. Therefore, wider ranges of temperature and S/F, as well as different bed materials can be tested.

Given the narrow operating window of commercial DFB gasifiers, it is difficult to define which of the operational and design choices contribute to efficient functioning. This is further complicated by inconsistencies in the reported data. For instance, most gasification data are reported in terms of concentrations, without closure of the carbon balance, and are derived using different tar quantification methods. In addition, the reported gas concentrations from commercial gasifiers contain some fraction of the inert gases added to the fuel feeding system. For instance, flue gases from the combustion side are used in the fuel feeding system of the Chalmers gasifier, which explains the presence of N_2 in Table 4. Overall, a comprehensive understanding of the influences of operating conditions requires a systematic and consistent evaluation of the raw gas composition, which would enable comparisons of cases. Therefore, in this thesis, an effort is made to close the carbon balance and validate the methods applied to characterize the raw gas (see Section 4.1).

Moreover, establishing the importance of design choices and operating parameters, such as mixing and ash-induced effects, is relevant to large-scale plants and long operating times, which are difficult issues to tackle at the laboratory scale. These questions can be addressed appropriately at the scale of the Chalmers gasifier (2–4-MW_{th}), which provides outcomes that are directly transferable to large DFB units.

Table 4. Selected information of DFB gasifiers in Europe with thermal capacities >1 MW.

DFB Gasifier (capacity)	Start-up year	Fuel type	Temperature	S/F (kg/kg$_{daf}$)	Bed material(s)	Tar in dry gas (g/Nm^3)	Dry gas^{a,b} (%vol)	Products	Status
Chalmers (2–4 MW$_{th}$)[d]	2007	Wood pellets	C: 820°–900°C G: 700°–850°C	0.7-1	Various	Benzene=6 Toluene=3 Styrene=0.5 Phenol=0.3 Indene=0.5 Naphthalene=1 Acenaphthylene=0.04 Phenanthrene=0. Other PAHs (≥4-ring)=0.2	H$_2$: 40^d CO: 14 CO$_2$: 30 CH$_4$: 6 C$_2$H$_4$:2 N$_2$: 4^c	Research only	Operational
Burgeis (2 MWth)	2012							0.5 MW$_{el}$	On hold
Alkmassr (4 MW$_{th}$) [29]	planned								Planned
Güssing (8 MW$_{th}$) [30]	2001	Wood residues	C: 930°C G: 850°–870°C		Pre-calcined Austrian olivine	Gravimetric=2 GC-MS=2	H$_2$: 42 CO: 23 CO$_2$: 20 CH$_4$: 9 C$_2$H$_4$: 3 N$_2$: n.r.	2 MW$_{el}$ 4.5 MW$_{th}$	End of demonstration lifetime reached
Oberwart (8.5 MW$_{th}$) [31]	2007	Wood chips	C: 940°C G: 850°C	0.5-0.6	Pre-calcined Austrian olivine	Gravimetric= 2 GC-MS=8	H$_2$: 38 CO: 25 CO$_2$: 21 CH$_4$: 10 C$_2$H$_4$: 2 N$_2$: 2	2.4 MW$_{el}$ 4.1 MW$_{th}$	On hold/Maintenance
Senden (15 MW$_{th}$) [32]	2011	Logging residues, wood chips	C: 950°C G: 850°C	0.9-1	Pre-calcined Austrian olivine	Gravimetric tar=0.4-1.0 GC-MS=17-10 Benzene=n.r. Toluene=n.r. Styrene=0.7-1.0 Phenol <0.2 Indene=2-3 Naphthalene=4-6 Acenaphthylene=1-3	H$_2$: 36-39 CO: 22-24 CO$_2$: 21-22 CH$_4$: 10-11 C$_2$H$_4$:3-4 N$_2$: n.r.	5.1 MW$_{el}$ 6.4 MW$_{th}$	Operational

10

Plant	Year	Feedstock	Temperature	[c]	Steam-to-fuel ratio[c]	Bed material	Tar composition[b] (g/Nm³)	Gas composition[a] (vol%)	Power	Status
Villach (15 MW_th)	2010		n.r.	n.r.	n.r.	n.r.	Phenanthrene=0.1–0.2 Other PAHs (≥4-ring)=0.2–0.4	n.r.	3.9 MW_el 6.7 MW_th	On hold
GoBiGas (32 MW_th)[d] [33]	2015	Wood pellets, wood chips, bark	C: ~900°C G: 830°–870°C	0.8	Norwegian olivine		Benzene=13 Toluene=0.5 Styrene=0.1 Phenol <0.2 Indene=0.2 Naphthalene=3 Acenaphthylene=0.5 Phenanthrene=0.4 Other PAHs(≥4-ring) =0.2	H₂: 39-41 CO: 21-24 CO₂: 20-26 CH₄: 8-9 C₂H₄: n.r. N₂: n.r.	20 MW_SNG	End of demonstration

[a] Dry gas composition as measured at the exit of the gasifier. They contain some minor fraction of an inerting gas, which is typically used for the fuel feeding system. This accounts for the presence of N_2 in some cases and part of the differences in the CO_2 content.

[b] The balance to 100% comprises other non-reported species, most likely minor hydrocarbons (e.g., C_2H_6, C_3H_6, C_3H_8), and probably N_2 used for inerting the fuel feeding system in some cases.

[c] From inerting gas to fuel feeding system. The inerting gas used in the Chalmers gasifier is dry flue gas from the combustion side, which typically contains 5% O_2, 72% N_2, and 23% CO_2.

[d] The gas and tar compositions for the Chalmers gasifier relate to operational conditions of 830°C in the gasifier, 890°C in the combustor, steam-to-fuel ratio of 0.8, and Norwegian olivine as the bed material.

[e] Typical tar composition at gasifier temperature of 830°C with wood pellets and Norwegian olivine as bed material.

n.r.=not recorded

2.1 The relevance of gas-solids mixing

In DFB biomass gasifiers, the extent of mixing of volatiles with bed material particles is assumed to be a crucial limiting factor for the catalytic conversion of volatiles, and this assumption is tested in this thesis. Traditional design choices aimed at improving gas-solids contacts include: the characteristic slope of the fuel feeding wall in the Repotec design (e.g., [32, 33]); a preference for in-bed fuel feeding over on-bed feeding (e.g., [34]); and the addition of internals in the freeboard of the gasifier (e.g., [35]). Increasing reactor complexity increases the risk for operational problems and higher maintenance costs. For instance, the use of in-bed feeding in the GoBiGas plant resulted in blockage of the fuel feed due to tar depositions, which were caused by excessive heat transfer to the screw feeder followed by partial devolatilization of the fuel [33]. This work gives the reference values for volatiles conversion when no design changes are made towards the goal of enhancing gas-solids mixing. The main differences in geometry and fuel feeding position between the typical Repotec design applied in the GoBiGas and Senden plants and that of the Chalmers gasifier are shown in Figure 8.
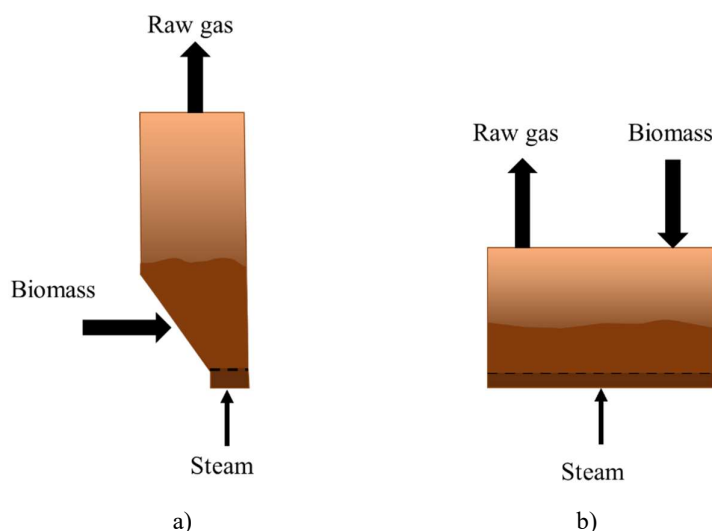

Figure 8. Examples of gasifier reactor geometry in DFB systems: a) Repotec design with in-bed feeding; b) Chalmers design with on-bed feeding.

In-bed feeding enhances volatiles-bed contacts when the time-scales for devolatilization and vertical dispersion are similar [19], and this is rarely the case in commercial DFB gasifiers. For typical biomass particles applied in industrial gasifiers (e.g., large and light commercial wood pellets/chips), the devolatilization time is longer than the time for rising through the bed [26]. This means that significant release of volatiles in the freeboard occurs regardless of the feeding position, which accords with the limited impact of the fuel feeding position on biomass gasifiers operated with catalytic bed materials [33, 34]. In the present work, fuel with a high floating tendency is used, i.e., commercial wood pellets. Therefore, the application of on-bed feeding (as in this work) or in-bed feeding is not expected to influence the results significantly.

Furthermore, fluidization velocity is a relevant operating parameter for bed-fuel mixing. It has been proven that under cold conditions (i.e., without release of volatiles), there is an optimal value of the fluidization velocity that results in maximum mixing of the fuel and bed material particles [36]. A higher fluidization velocity intensifies the ejection of particles into the freeboard [37], which favors contacts between the volatiles and bed material particles in the splash zone and the freeboard. For instance, in the Senden gasifier, the addition of fluidization nozzles at the fuel feeding position resulted in enhanced conversion of volatiles [32], which may indicate that poorly fluidized regions are located around the tilted wall of the gasifier (*cf.* Figure 8b).

Paper I aims to elucidate the extent of the contacts between the bed material and the volatiles released from the fuel in a freely bubbling bed with over-bed feeding, and the relation to fluidization velocity. The impact of fluidization on fuel conversion is further investigated with catalytic materials in **Paper III**.

2.2　Steam-to-fuel ratio

There are indications that the steam concentration exerts a limited influence on biomass conversion at the relatively high S/F that are commonly applied in large steam gasifiers. At steam concentrations >0.5 $kg_{steam}/kg_{dry\ biomass}$, increasing the S/F yields an increase in the concentrations of H_2 and CO_2, with this effect moderating as the steam concentration increases. This is attributed to a combination of enhanced WGS reaction and steam reforming of condensable species [38, 39]. Steam has been found to promote the decomposition of the non-aromatic oxygenated condensable species [12, 40], while the yield of aromatics remains relatively stable compared to a pyrolysis case without steam. This is in line with the literature on steam cracking of non-oxygenated feedstocks (e.g., naphtha), which considers steam as an inert species that is applied to dilute the feedstock [16]. In terms of char conversion, increasing the steam concentration to >60% does not seem to affect the rate of char gasification [41].

Given the expected weak effect of steam on fuel conversion at high steam concentrations, the influences of secondary variables that have been modified unintentionally can assume importance, e.g., the residence time of the gases in the reactor, and the gas-solids contacts. The combined effect of S/F, residence time, and gas-solids contacts are explored in **Paper II**, whereby an inert bed material and an active bed material are applied with the ambition to minimize and maximize the bed-volatiles interactions, respectively. With an inactive bed, the effect of increasing the steam flow was mainly manifested as a shortening of the residence time of the gas in the reactor; whereas with an active bed, the effect of the higher flow of steam was mainly attributed to enhanced volatiles-bed material interactions. Additional investigations of the effects of steam flow when using different active bed materials are shown in **Paper III**.

2.3　Choice of active bed material

The catalytic materials applied in DFB gasifiers should be robust and able to withstand high concentrations of steam, continuous input of ash species, and frequently alternating oxygen-rich and fuel-rich atmospheres. In such environments, commercial Ni-based steam reforming

catalysts are likely to fail due to poisoning [42]. Thus, less-expensive naturally occurring materials with resistance to agglomeration are preferred in commercial gasifiers [43]. However, this entails a compromise in relation to the higher catalytic performance that a synthetic catalyst provides. Typically, the major indicator of the catalytic activity of the bed materials in DFB gasifiers is the tar reduction ability, which is usually assessed by comparisons to other materials.

Catalytic function. Transition metals, which are steam reforming catalysts [18], e.g., Fe, can be found at different concentrations in natural materials. As shown in Figure 9, for the materials used in this work, the concentrations of transition metals range from below 0.1% for silica sand and feldspar to more than 40% for ilmenite and manganese ore. Except in the case of manganese ore, iron is the predominant transition metal in the materials used. In the gasification environment, Fe has catalytic activity towards steam reforming, tar decomposition, and the WGS [44, 45]. Therefore, some steam reforming capability can be expected for all these materials in relation to their iron content.
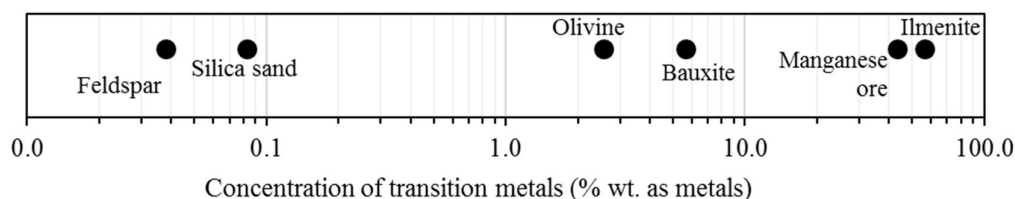

Figure 9. Total concentrations of transition metals in the bed materials applied in this work. Transition metals found in the original composition of the materials include Fe, Mn, Ti, and traces of Cr and Ni. Values shown are %wt., recalculated as elemental species.

Oxygen carrier function. A limitation linked to the use of transition metal-based catalysts in DFB gasification is their ability to transport oxygen from the combustor to the gasifier in the form of reducible oxides. For iron, this occurs via the redox cycle, summarized in Reactions 5–7 [46]. Oxygen-carrying capacity is the basis of the Chemical Looping Combustion (CLC) technology, and it enhances the rate of char conversion under CLC conditions [47, 48], and promotes tar oxidation [21, 49]. However, oxygen transport also leads to the oxidation of valuable syngas species [50], which enriches the raw gas in combustion products (i.e., CO_2 and H_2O) to the detriment of CO and H_2. In synthesis applications, oxygen transport in the gasifier requires energy-intensive CO_2 separation before the synthesis step [51, 52].

Table 5. Redox cycle experienced by iron oxide when alternating between the combustion and gasification sides of a dual fluidized bed gasifier.

	(R5)	Combustion side
$4FeO + O_2 \rightarrow 2Fe_2O_3$		
$Fe_2O_3 + H_2 \rightarrow 2FeO + H_2O$	(R6)	Gasification side
$Fe_2O_3 + CO \rightarrow 2FeO + CO_2$	(R7)	Gasification side
$H_2 + CO + O_2 \rightarrow H_2O + CO_2$	(R8)	Net reaction

Papers III and **V** relates the raw gas composition to the choice of bed material. The ambition is to map the main effects induced by the bed material on fuel conversion, i.e., the dominant catalytic, oxygen transport, and thermal effects.

2.4 Bed material circulation rate and char conversion

The circulation rate affects the outcome of the gasifier in two different ways: (1) it influences the residence time of the fuel/char particles in the gasifier; and (2) it contributes to the ratio of the flows between the active bed material and fuel. Yet, this parameter is commonly overlooked or ignored, and it is seldom reported in the gasification literature. This is most likely due to the fact that the circulation rate is the combined result of other operating parameters in a DFB unit, such as gasifier geometry, bed material properties, and temperature. As a consequence, it is difficult to quantify.

For CLC applications, different correlations (as well as lack of correlation) between the circulation rate and fuel conversion rate have been reported in the literature, which indicates an interplay of opposite effects. For instance, higher rates of solids circulation can lead to a lower rate of char conversion due to the shorter residence time [53], or a higher rate of char conversion owing to the overall less-depleted and more-reactive oxygen carrier material [54]. The ratio of the flows of oxygen carrier and fuel is usually evaluated as a stoichiometric ratio of oxygen (ϕ). Two different operating windows are suggested in the literature [53]: at low oxygen transport (i.e., $\phi<3$), a higher circulation rate is beneficial to increase fuel conversion; while at $\phi>3$, the influence of the circulation rate on char conversion is limited.

The impact of the solids circulation rate on char gasification is investigated in **Paper V** for a strong oxygen carrier such as ilmenite, which is representative of CLC operation; and for a moderate oxygen carrier, which is representative of the gasification conditions in **Paper IV**.

2.5 Temperature and polyaromatic growth

The choice of temperature in DFB gasifiers (i.e., 850°–900°C) is traditionally based on the principle that operating at a high temperature is beneficial for obtaining a high yield of gas [8], as long as the bed material can tolerate this temperature, e.g., avoid agglomeration. This *rule of thumb* warrants reconsideration in the case of catalytic materials being applied, as the conversion rates are enhanced by the catalyst. A lower operating temperature also limits secondary undesired reactions, such as polyaromatic growth species [5, 17, 55]. This issue is explored in **Paper VII**.

With increasing temperature, both aromatic [56] and non-aromatic [57, 58] nascent volatile species can contribute to the formation of heavy tar, as schematized in Figure 10. Once the aromatic rings are formed, they are difficult to open at the temperatures typically used in DFB gasifiers (<900°C) [5]. Nevertheless, aromatic species continue to react, forming new aromatic species and permanent gases. For instance, CO is a major product of the thermal decomposition of phenol [59]. Dealkylation of alkyl-aromatics represents a source of light hydrocarbons (and condensed rings), e.g., methane and benzene are usually produced as a result of the dealkylation

of toluene [60, 61]. These thermally induced reaction paths are in line with the decrease in number of tar species at higher temperatures, where benzene and other non-substituted aromatics, such as naphthalene, are the most predominant species [62].
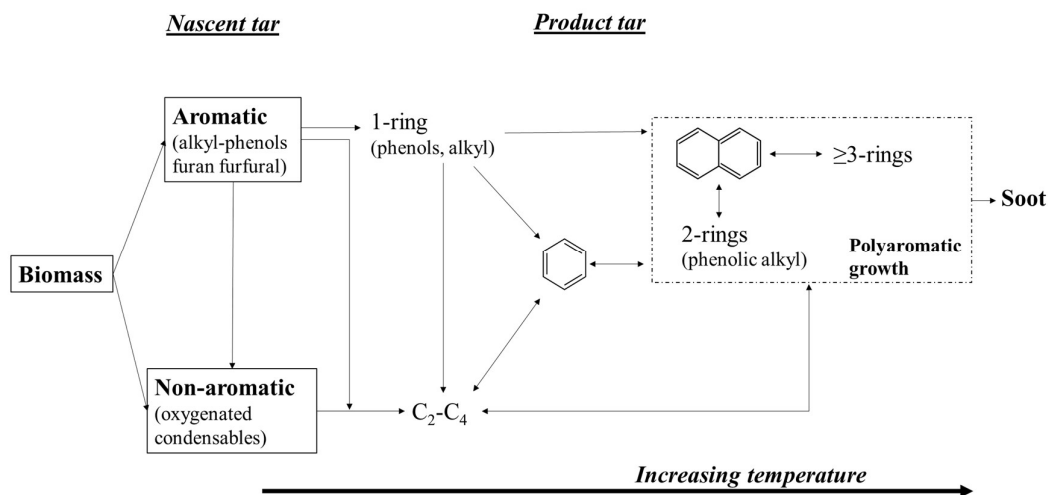
Figure 10. Simplified schematic of the contributions of aromatic and non-aromatic nascent tar vapors to the growth of polyaromatic species with increasing operating temperature. Only hydrocarbons are included in the schematic. Elaborated from refs [5, 55-60, 62-64]

Further growth into larger polyaromatic species occurs through various mechanisms, which involve radical chain reactions and hydrogen abstraction as a necessary step to generate radicals. Acetylene [63], cyclopentadienyl/indenyl, and phenyl radicals [64] have been proposed as key intermediates in the polymerization reactions. Figures 11- 12 show examples of naphthalene and acenaphthylene formation according to these mechanisms.
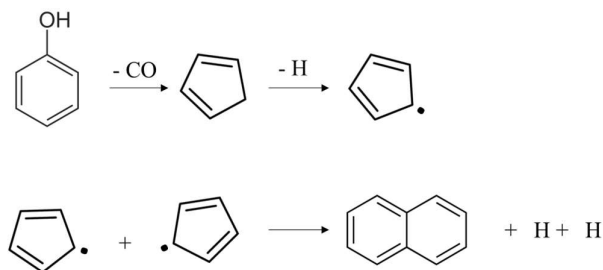
Figure 11. Formation of naphthalene via cyclopentadienyl addition.[64]

16
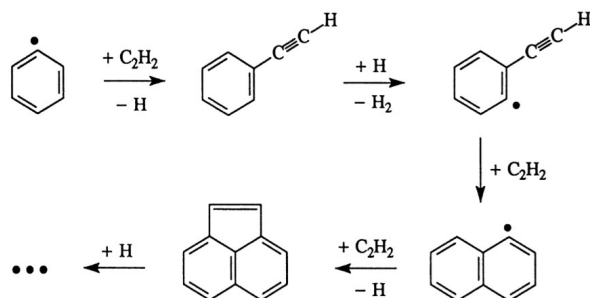
Figure 12. Formation of acenaphthylene according to the H-abstraction C_2H_2 addition mechanism [63].

The chemistry of polyaromatic growth has been traditionally described in terms of combustion chemistry [65]. Due to similarities of the conditions between fuel-rich flames and gasification, analogous polyaromatic growth mechanisms can be expected. However, the extent of polymerization is influenced by the concentration of H_2, which is higher in gasifiers (~20%–60%). In an investigation conducted by Jess [60], 48% H_2 decreased the conversion of naphthalene by half, as compared to a case without hydrogen (1100°C and 1s). A higher H_2 concentration also resulted in lower production of soot. This is thought to occur via termination reactions that involve H_2 [60, 66].

3 - Influence of biomass ash on the performance of DFB systems

3.1 Influence of ash species on bed material activity

In contrast to the experience with traditional steam reformers, the inorganic impurities in the fuel benefit the catalytic activities of natural bed materials used in DFB gasifiers by forming an active ash layer, e.g., on olivine [30, 67], bauxite [68] and, in the present work, feldspar [69] particles. Among the main inorganic species found in biomass (Ca, K, Na, Mg, S, Si, P, Al and Cl [70]), Ca and K have attracted the most attention for their relatively larger shares in biomass ash (e.g., 10% K and 20% Ca in pine wood) and for their catalytic activities. This has encouraged the use of Ca, and more recently K-rich additives to enhance and control the activity of the olivine bed material in existing gasifiers, e.g., additions of K_2CO_3 and limestone in the GoBiGas plant [9] and of CaO and limestone in the Güssing plant [71].

However, the active phase(s) and catalytic mechanism(s) of the ash layer on the bed material particles in DFB gasifiers remain unclear, and the situation is further complicated by the addition of various additives. In the case of olivine, heterogeneous catalysis by Ca-species have been suggested to play an important role, based on the abundance of Ca in the ash layer [30]. The addition of K results in mixed Ca-K oxides, which can participate in the oxidation of hydrocarbons via an oxygen loop between the combustor and the gasifier [72]. In addition, it has been proposed that gas-phase catalytic interactions occur by means of potassium uptake/release cycles driven by the different gas atmospheres in the DFB [67, 73]. In such cases, S-additives could contribute to the activity of the bed material by fixing K in the ash layer in a releasable form. This hypothesis is in line with the uptake/release cycle described previously [67], whereby K_2SO_4 can form in the combustor and decompose into catalytically active KOH (g)/KCO_3 (g) in the reducing zones of the gasifier. The addition of S to enhance the catalytic activity of the bed is tested in **Paper IV** for olivine.

3.2 Flows of inorganic species in DFB systems

The accumulation and transport of ash species in a DFB system occur in different manners depending on the compositions of the fuel ash and the bed material applied. As schematized in Figure 13, K, Na, Cl, S, and P have higher tendencies to be released from the fuel as vapors, as compared to Al, Ca, Mg, and Si which tend to remain in solid form [74, 75]. A higher content of Si in the form of free SiO_2 in the bed material or the ash contributes to the bonding of alkali in non-volatile silicates, while Ca enhances the release of K by reacting with the existing Si [76, 77].

When SiO_2 and alkali are highly available in the DFB system, the formation of alkali silicates can cause bed agglomeration problems owing to the formation of low-melting-temperature

19

silicates [78], e.g., with silica sand beds and alkali-rich fuels. In such cases, the bed material is regularly replaced to minimize the risk of severe agglomeration. With bed materials that have lower Si contents than that of silica sand, melts are thought to trigger the formation of the active ash layer and facilitate further reactions with solid species in the bed, as indicated by the arrows pointing towards the bed material in Figure 13. For instance, this enables the incorporation of Ca into the olivine [79] and feldspar [80] structures.
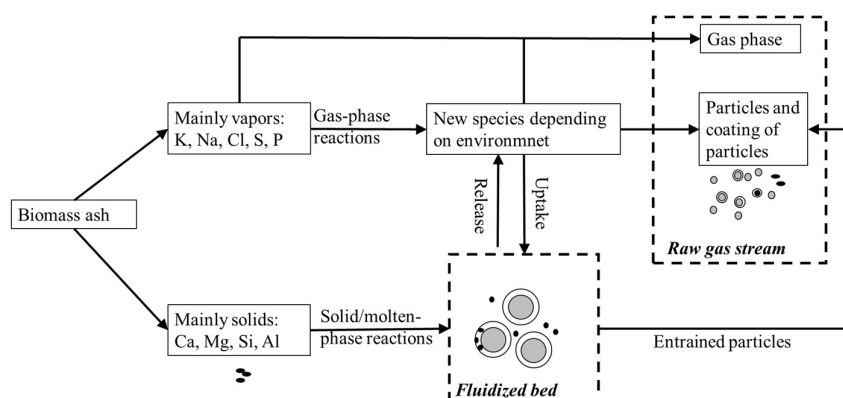
Figure 13. Simplified scheme for the fates of ash-forming species in a biomass gasification reactor.

Depending on the sizes of the ash input and outputs, an excessive loss of catalytically active inorganic species can occur. Inorganic compounds exit the DFB with the raw gas and/or the flue gas, in the forms of gaseous species or entrained particles, as shown on the right-hand side of Figure 13, that will be collected in filters. For instance, the net transport of sulfur [43] and potassium [81] from the combustor to the gasifier, with subsequent loss by the raw gas stream, have been observed in the Chalmers and Güssing DFB units, respectively. The excessive loss of inorganics is partially compensated by the recirculation of ashes in external loops (Figure 14), as is the case in the existing gasifiers in the GoBiGas (32 MW) [33], Güssing (8 MW) [81], and Senden (15 MW) [82] plants.

Figure 14. Ash flows in a DFB gasifier (as described in [81]).

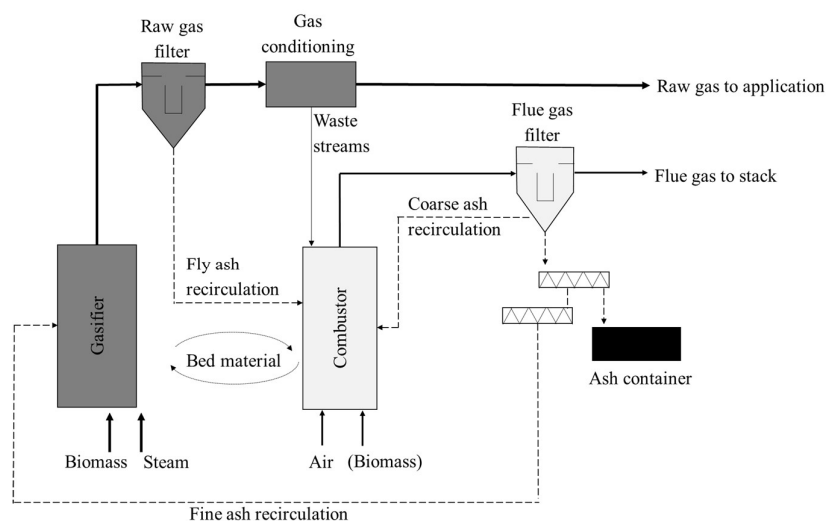The practical application of ash recirculation for the purpose of sustaining the catalytic activity in large DFB gasifiers has been addressed recently in the literature [32, 83]. However, to date, the primary application of ash recirculation in gasifiers has been for the recovery of unconverted carbon in the fly ash. Furthermore, coarser ash, which is rich in bed material particles, can also be recirculated with the aim of minimizing bed material loss in the system [32, 81]. Results showing the catalytic effect of the ash streams in the gasifier are also presented in this thesis.

3.3   Influence of the ash layer on char conversion

The char gasification rate is catalyzed by the presence of alkali and alkali earth metals (AAEM) [84-86], and the ash layer is a potential source of those catalytic species. The hypothetical transfer of catalytic ash species from the ash layer to the char matrix can occur as follows: (1) solid particles rich in refractory species, e.g., Ca and Mg [87], are trapped into the char matrix; or (2) as gaseous alkali-rich compounds released from alkali-containing phases in the bed material [77, 88, 89]. The transfer of gaseous alkali from the bed material to a char particle has been demonstrated by Keller et al. [90] under CLC conditions, and using an oxygen carrier material (manganese ore) pre-soaked in K_2CO_3. The enhanced gasification rate was partially attributed to the transfer of K from the bed to the char in the form of KOH(g). **Paper VI** extends the study of Keller et al. [90] to examine the interaction of ash-coated materials with char, in particular to olivine that has been activated by the in-bed addition of K and S.

3.4   Influence of the ash layer on gas and tar conversion rates

The heterogeneous catalytic action of the ash layer towards selected hydrocarbons has been shown by Kuba et al. [91, 92], whereas homogeneous interactions have not been directly addressed in the gasification literature. Nevertheless, there are indications that gas-phase tar chemistry can be altered by the presence of AAEM under gasification conditions. The potential interactions of AAEM with the tar chemistry in DFB gasifiers are summarized in Figure 15.

AAEM can prevent polyaromatic growth in an indirect manner by increasing the concentration of H_2 [60, 66, 93], as a result of the catalytic destruction of tar [93] and/ the catalyzed WGS equilibrium [30, 67, 68]. Catalytic reforming of tar precursors can also prevent further polymerization, as observed by Kuba et al. [92], who identified reduced polymerization of indene into chrysene in the presence of an ash-layered olivine. Furthermore, direct interactions between volatile alkali and the tar chemistry have been suggested [94-96]. For instance, Hindiyarti et al. [95] have described how KOH and atomic K terminate hydrogen and hydroxyl radicals, which are involved in the gas-phase reactions of hydrocarbons [97]. The influence of K in the radical chemistry is very sensitive to the operating conditions [95], i.e., temperature and gas composition, and its relevance to tar growth under conditions relevant for steam gasification remains unexplored.
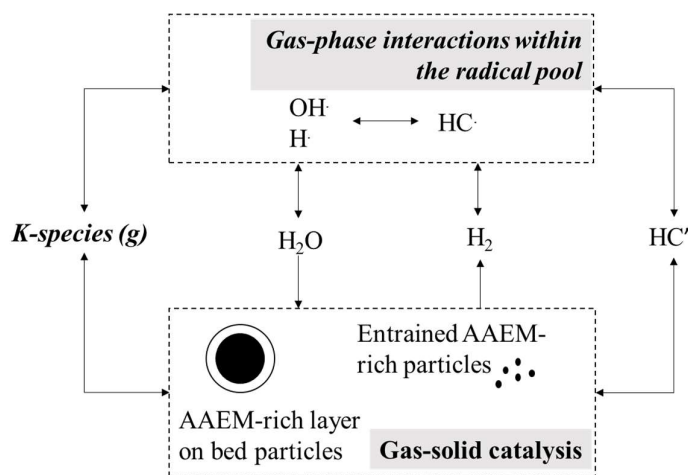
21

Figure 15. Potential interactions between AAEM and tar chemistry in DFB gasifiers. HC′ represents a generic hydrocarbon, and HC• represents a generic hydrocarbon radical. Elaborated from refs [60, 66, 91-96]

Additionally, with in-bed catalysts, the AAEM in the ash layer are exposed to the reactive nascent tar precursors. Although the literature on the influence of AAEM on the gas-phase cracking of oxygenated hydrocarbons is scarce, it indicates that nascent oxygenated vapors are more heavily influenced by AAEM than aromatic species. For instance, the formation of carbon oxides and lighter gases to the detriment of condensable species in the presence of AAEM-salts is more pronounced for cellulose-derived vapors than for lignin-derived vapors [98]. Recently, Jiang [96] confirmed that gas-phase K promotes steam reforming of cellulose-derived vapors in the temperature range of 500°–900°C. These early interactions of oxygenates and the bed material can be crucial with respect to the tar reduction ability with in-bed catalysts, as suggested by Corella et al. [99]. However, a detailed tar composition was not available to confirm their suspicions. Further catalytic destruction of aromatic tar species is likely to occur, as shown by Kuba et al. for indene and toluene, where a 3-fold increase in reactivity was facilitated by ash-layered olivine, as compared to fresh olivine material [91, 92].

Paper VII explores the catalytic action of an ash-layered olivine on tar conversion when applied as a bed material in the gasifier, with the ambition to elucidate the tar reduction pathways (s) promoted by the ash-coated olivine.

4 - Experimental section

4.1 Carbon balance and definitions

The main analytical tool used in this thesis is the carbon balance over the gasifier reactor, which is considered a prerequisite for ensuring the quality of the experimental data and to extract reliable conclusions about the fuel conversion. The total carbon in the raw gas is here divided into three groups of carbon-containing species according to the quantification methods applied: permanent gas ($n_{C,PG}$), which is determined by gas chromatography; aromatic species ($n_{C,SPA}$), determined by the Solid Phase Adsorption (SPA) method [100, 101]; and unidentified condensable species ($n_{C,UCS}$), which are not covered by the previous methods. The species quantified using the methods applied here are summarized in Figure 16 .
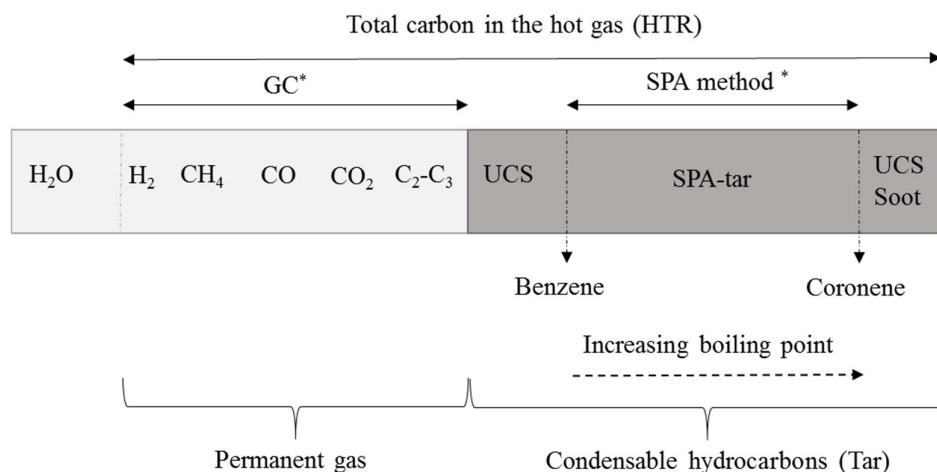
Figure 16. Raw gas spectrum and measurement methods. * Species covered by the method applied in the present work. PG, permanent gas. SPA, solid phase adsorption. HTR, High Temperature Reactor applied in this work to quantify the total carbon in the hot raw gas. UCS, unidentified condensable species, which are determined by difference.

To quantify the total carbon in the hot raw gas, an independent measurement is introduced. This is based on a High-Temperature Reactor (HTR) [102], where the hot raw gas is completely converted into CO_2, CO, H_2O, and H_2. These species are readily measured by gas chromatography, and the total carbon in the hot gas ($n_{C,HTR}$) can subsequently be calculated.

4.2 The Chalmers gasifier

The DFB unit at Chalmers consists of a 2–4-MWth gasifier coupled to a 12-MWth boiler; a simplified sketch of the system is depicted in Figure 17 with the parts numbered. The gasifier has a cross-sectional area of 1.44 m^2 and it operates in the bubbling regime, while the boiler is a circulating fluidized bed (CFB) with a cross-sectional area of 2.1 m^2 and a height of 14 m.

The typical operating conditions of the DFB system are 810–820°C in the gasifier bed, 850°C in the bottom bed of the boiler, and sub-atmospheric pressure of 1–2 kPa.

The system can be operated in two different modes: only-boiler mode; and gasifier-mode. During boiler operation, the bed material by-passes the gasifier and flows directly from the particle distributor (5) back to the combustor (1). During gasification operation, the circulation of bed material between the reactors is enabled by fluidizing the inlet and exit loop seals (7-8), the gasifier (6), and the particle distributor (5). The return of the bed material from the gasifier to the boiler is represented by a red circle in the figure.

Fuel feeding to the gasifier is only allowed in the presence of operating staff, which limits the gasifier experiment to the hours of approximately 6 am to 6 pm. Outside of that period and during the weekends, the bed material continues to circulate through the gasifier, with flue gases as the fluidization agent, and fuel is fed only to the boiler side. The boiler is fed with fuel without interruption throughout the winter season to provide heat to the Chalmers campus.

1. Furnace
2. Fuel Feeding (Furnace)
3. Wind Box
4. Cyclone
5. Particle Distributor
6. Gasifier
7. Loop Seal 1
8. Loop Seal 2
9. Fuel Feeding (Gasifier)
10. Raw gas line
11. Raw gas sample
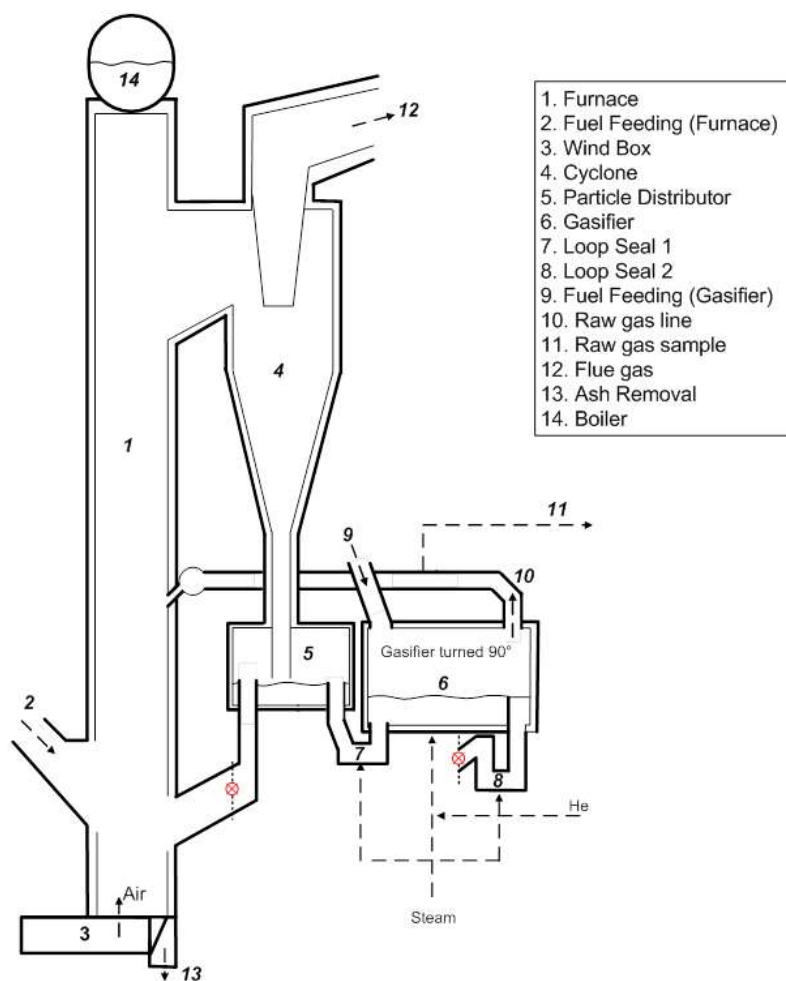12. Flue gas
13. Ash Removal
14. Boiler

Figure 17. Schematic of the Chalmers DFB gasifier.

During gasification experiments, the gasifier is fluidized with steam, which is fed through nozzles located at the bottom of the bubbling bed. The fuel is fed by gravity via the fuel chute (9). The fuel feeding rate is controlled by the rotation speed of the screw feeder, and it is led into the gasifier by a system of rotary valves with the function of an airlock. A small stream of dry flue gases from the boiler is used as a purge gas in the rotary valve system to prevent air from entering the gasifier.

The recirculation of inorganics in the Chalmers system occurs through the return of the raw gas stream to the combustor (see line 10 in Figure 17). This reproduces the regular recirculation of fly ash streams in commercial DFB gasifiers. The combustion of the raw gas in the combustion side is suitable for research purposes, whereas in a commercial unit the raw gas would go through the gas cleaning steps and, thereafter, proceed to the final application or further processing.

When the influence of ash streams on bed activity is investigated, the ash stream collected in the secondary cyclone (after position 12 in Figure 17) is reintroduced into the loop seal at the inlet of the gasifier (8 in Figure 17). This ash stream contains entrained bed material and ash particles that were not separated by the primary cyclone (4).

4.3 Fuel and bed materials

All the gasification experiments presented in this thesis are carried out with wood pellets. In the boiler side, wood chips or mixtures of wood chips and pellets are usually applied. The elemental composition of the fuels is analyzed by the Research Institutes of Sweden (RISE) using the standard methods listed in Table 6. The moisture content is analyzed in-house by gravimetric analysis of fuel samples before and after drying the sample at 105°C for 24 h in an oven. Variations in the fuel composition relate to the natural heterogeneity of the fuel. Nevertheless, the variations fall within the accuracy of the analysis method applied by RISE, and the fuel is, therefore, considered the same across campaigns.

Table 6. Range of compositions of the wood pellets fed to the gasifier and wood chips used in the boiler, during the experiments described in this thesis. The moisture measurement was carried out at Chalmers, while the ultimate analysis was performed by RISE.

Parameter	Wood pellets	Wood chips	Unit	Method
C	50–51	49–50	mass% db	SS-EN-ISO 16948
H	6.0–6.2	6.0–6.2	mass% db	SS-EN-ISO 16948
O	43–44	43	mass% db	By difference
N	0.05–0.07	0.11–0.13	mass% db	SS-EN-ISO 16948
S	<0.02	<0.02	mass% db	SS-EN-ISO 16994
Cl	<0.01	<0.01		SS-EN-ISO 16994
LHV	18.9–18.5	18.7–18.3	MJ/kg db	ISO-1928
Ash	0.4–0.5	0.5–0.7	mass% db	SS-EN-ISO 18122
Moisture	6–10	36–46	mass%	By difference between the wet and dry samples

Approximately 90% of the ash input to the Chalmers DFB during a day of gasification experiments originates from the fuel fed to the boiler side. This is a result of the relatively higher fuel flow and longer operational time of the boiler, as compared to those of the gasifier. The typical ash compositions of the wood chips and pellets are summarized in Figure 18, where Ca and K are found to be the most abundant species. The K/Si molar ratio of the wood pellets corresponds to the stoichiometric ratio of K_2SiO_3 (2.0±0.4 mol K/mol Si), while there is an excess of K with respect to Si in the case of wood chips (5.6±1.6 mol K/mol Si). Ca is in excess with respect to Si for both fuels, i.e., 4.3±0.7 mol Ca/mol Si for the wood pellets and 9.2±2.7 mol Ca/mol Si for the wood chips.
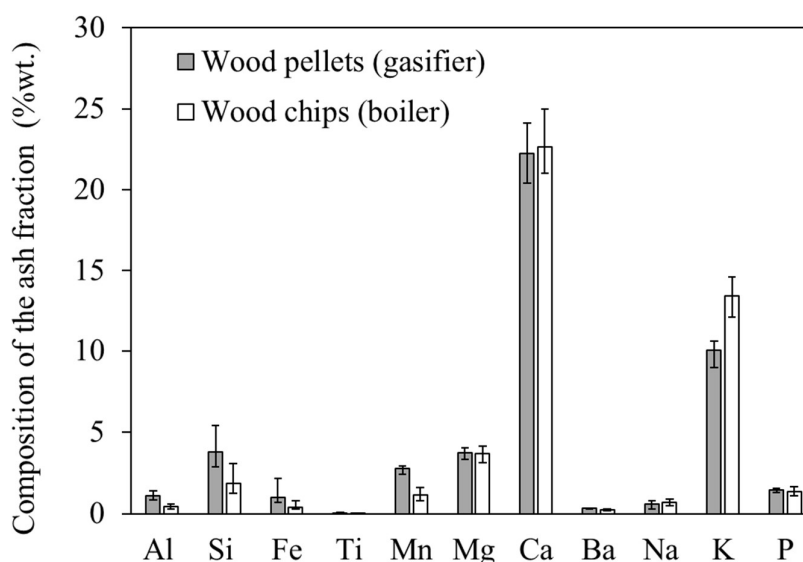

Figure 18. Compositions of the ash fractions of the wood pellets and chips. Shown are the average and standard deviation of the ash compositions of the wood pellets and chips applied over the different experimental campaigns included in this thesis.

Six different bed materials have been tested in this thesis; silica-sand; ilmenite sand; bauxite; olivine; alkali-feldspar; and a manganese ore. The estimated fluidization-related properties of the materials are listed in Table 7, and their chemical compositions (as provided by the supplier) are summarized in Table 8. The supplied ilmenite, manganese, and feldspar materials had smaller particle sizes, as compared to those of the silica sand, olivine, and bauxite. As a consequence, for the range of flows of fluidization steam that were possible in the experimental setup (100–360 kg/h), the fluidization ratios (u_o/u_{mf}) were comparatively higher for ilmenite, feldspar, and manganese.

Table 7. Physical and estimated fluidization properties of the materials tested.

	Silica sand	Olivine	Bauxite	Ilmenite	Feldspar	Manganese
Particle density (kg/m^3)[b]	2650	3300	3000	4200	2600	2600
Mean diameter, d_p (µm)	316	288	305	195	180	185
Minimum fluidization velocity[a], u_{mf} (m/s)	0.04	0.05	0.05	0.03	0.02	0.02
Range of fluidization number tested[a], u_o/u_{mf}	3–4	2–6	3–4	3–10	11	9–19

[a] Based on the flow of steam at the average bed temperature.

[b] As given by the supplier.

The expected fraction of SiO_2 that is readily available to bond permanently AAEM from the fuel ash components is comparatively higher for silica sand. Based on stoichiometric considerations, the fraction of free SiO_2 is 99.2% for silica sand, and 0%–6.5% for the other five materials, as listed in the last raw of Table 8. In the case of feldspar, the Si content is high, although 91% of the Si is in the form of aluminosilicates and only 9% is in the form of free SiO_2, according to the supplier.

Table 8. Chemical composition (%wt.) of the materials tested, and estimated levels of free SiO_2 (%wt.)

	Silica sand	Olivine	Bauxite	Ilmenite	Feldspar	Manganese
SiO$_2$	99.2	41.7	6.50	0.40	67.5	7.95
Al$_2$O$_3$	0.17	0.46	88.50	0.35	18.8	6.42
Fe$_2$O$_3$	0.054	7.4	1.10	35.0	0.11	7.36
Ti$_2$O			3.0	51.0	0.01	0.392
MgO		49.6		1.00	0.04	0.418
Cr$_2$O$_3$		0.31		0.30		
NiO		0.32				
MnO$_2$				1.30	<0.0078	59.7
V$_2$O$_5$				0.23		
Na$_2$O					4.3	
K$_2$O					8.4	1.19
CaO				0.02	1.2	2.63
Estimated free SiO$_2$ [a]	99.2	0.0	6.5	0.0	6.0[b]	3.7

[a] Assuming all alkali and alkali earth metals are present in the form of silicates.

[b] As given by the bed material specifications.

4.4 Sampling methods

All raw gas measurements are conducted in two separate slipstreams (~10 Ln/min), which are sampled at the raw gas channel (11 in Figure 17) and after a hot gas filter, as shown in Figure 19. The filter and the sampling lines are heated to 350°C to avoid condensation of hydrocarbons. Slipstream 1 is used for sampling tar and permanent gases, whereas slipstream 2 is led to the High Temperature Reactor (HTR) for quantification of the total carbon (explained below).

He-tracing. A small flow (~20–50 Ln/min) of high-purity helium (99.996%) is used as a tracer gas for quantification of the total dry gas flow per unit of fuel. The flow of He is chosen so that the concentrations measured in the raw gas and at the exit of the HTR fall within the calibration range of the instrument, which is usually 0.2%–1%. Helium is added to the fluidization steam, as indicated in Figure 17, by a mass flow controller (Bronkhorst® model F-202AV). The He stream enables the quantification of the total yield of dry gas generated per unit of fuel.

Gas chromatography. The concentrations of He and permanent gas species in the slipstream 1 are analyzed in a micro-gas chromatograph (μ-GC). The slipstream is quenched with isopropanol and further cooled to remove water and tar before the stream enters the μ-GC, as shown in Figure 19. The μ-GC used was the Varian CP4900, which has two channels and uses Poraplot Q and MS5Å columns, with He and Ar as the carrier gases, respectively. The μ-GC takes a point-injection (10–30 ms injection time) of the dry and tar-free raw gas every 3 minutes, generating a new chromatogram from each injection. The μ-GCs is calibrated regularly (usually every week) with five concentrations levels that cover the range of expected concentrations. The species assayed are: H_2, He, CO, CO_2, CH_4, C_2H_2, C_2H_4, C_2H_6, C_3H_6, C_3H_8 and N_2.
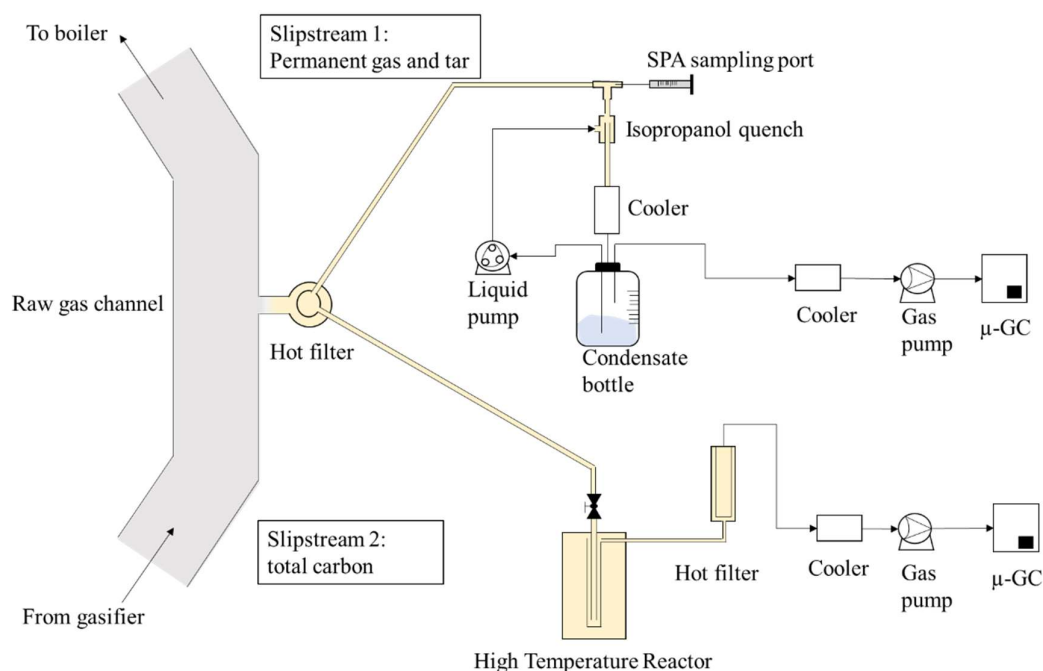

Figure 19. Simplified schematic of the gas sampling system, including the two parallel slipstreams, and the SPA-sampling position. The colored lines are the heat-traced line at 350°C. The remainder of the piping corresponds to the cold sides of the slipstreams.

High-Temperature Reactor (HTR). The HTR [102] consists of a ceramic tube reactor inserted into an electrically heated oven that is operated at 1700°C. A heated line (350°C) leads Slipstream 2 into the HTR. As shown in Figure 19, the gas at the exit of the HTR is passed through a hot filter to remove soot (if any), and then cooled to remove moisture before analysis in the μ-GC. The μ-GC is a Varian CP4900, with MS5Å and Poraplot U columns, and it uses Ar and He as carrier gases, respectively.

The proper functioning of the HTR to quantify the total carbon is assessed based on the CH_4 concentration and the formation of soot. Only measurements with zero CH_4 are considered successful, to ensure that the thermal severity is sufficiently strong to decompose all the hydrocarbons into simpler molecules (CO_2, CO, and H_2). Furthermore, the soot formation should be negligible, so as not to underestimate the total carbon. Any soot formed is collected in the hot filter and is quantified at the end of the experiment (when possible) by burning the soot with a known flow of air, followed by measurement of the gas composition. Satisfactory measurements typically result in a soot yield equivalent to <0.5% of the carbon in the fuel.

SPA-method. Tar samples are acquired according to the solid-phase adsorption (SPA) method [100, 101]. All SPA samples were collected with Supelclean ENVI-Carb/NH_2 SPE columns, except those taken during the bauxite tests, which were earlier experiments and were carried out with the less-efficient LC-NH_2 columns. The main advantage of the preferred Supelclean ENVI-Carb/NH2 columns is that they have 7–10-fold higher efficiency of adsorption of BTX (benzene, toluene, xylene) species, as compared to the LC-NH_2 columns.

For an SPA sample, 100 mL of hot gas is forced through the adsorbent column with the help of an automatic syringe. The SPA columns are eluted with a solvent, and the resulting sample solution is collected in a vial for analysis. The column is then washed a second time with solvent, and a control sample is produced to ensure that all the tar species have been extracted in the first elution step. Both vials (sample and control) are analyzed in a gas chromatograph equipped with a flame ionization detector (GC-FID). Three (repeat) chromatograms are generated per vial, generating up to six chromatograms per SPA column collected.

The GC-FID used is the BRUKER GC-450 and GC-430, and the temperature program is defined to detect species with boiling points between those of benzene and coronene. The instrument is calibrated for 28 tar species (listed in Table 9), and the calibration curves are built on five different concentrations of each one of these species. The accuracy of the GC-FID is tested at the beginning and at the end of the analysis of each SPA set by analyzing a known sample, i.e., an aleatory chosen calibration level. The analysis is considered satisfactory if the deviation of the known sample from the calibration level is less than 10% (rel).

4.5 Data evaluation and validation of the combined measurements

The results generated in this thesis have all been subjected to the same sampling, analysis, and evaluation procedures. Systematic errors are, therefore, expected to be similar for all the experiments, rendering the observed trends statistically significant. Random errors are minimized by carrying out repeat samples and, when possible, repeat experiments.

Unless otherwise specified, the results are shown as the average values derived from multiple measurements over a period of 30–60 min of stable operation, and the error bars indicate the variations of the results due to fluctuations of the process during that time. Here, stable operation means that the flows of fuel and steam are constant, and that the temperature fluctuates within ±3°C. Fluctuations of the fuel feeding system (due to pulses of fuel flow) and steam flow usually remain below 3% (rel) and 1% (rel), respectively. Additional fluctuations

due to the mixing conditions are also expected, e.g., steam bubbles and pulses of the bed material flow entering and leaving the gasifier.

The yields of permanent gas species represent the average of 10–20 chromatograms, which usually has a standard deviation of 0.3%–2.0% (rel) for the major gas components. The yields of tar species represent the average of 3–4 repeat samples, involving 18–24 chromatograms. Typically, the standard deviation among repeat SPA samples is <10% (rel), and for abundant species, such as benzene, toluene, phenol, and naphthalene, the deviation is generally lower, i.e., <5% (rel), as integration errors are less likely to occur for larger peaks.

Yields (g/kg daf fuel or mol/kg daf fuel) are calculated based on the He-tracing method and according to Equation 1, where n_i denotes the molar yield and C_i is the concentration of the species i. $\dot{V}_{He-tracing}$ and C_{He} are the flow and measured concentration, respectively, of the tracer gas. Yields are preferred to concentrations to avoid misinterpretation between a lower production of a species and the same level of production but a dilution effect due to higher generation of gas. However, concentrations are used when the levels are compared to those generated in commercial gasifiers, since the latter are usually reported in concentration units.

$$n_i = \frac{C_i}{\dot{m}_{daf,fuel}} \cdot \left(\frac{\dot{V}_{He-tracing}}{C_{He}} \right)$$

Equation 1

As a data visualization tool, the permanent gas is shown in a Van Krevelen-type of diagram (H/C vs O/C molar ratios) considering only the species CO, CO_2 and H_2, as proposed by Larsson et al. [3]. In an H/C-H/O diagram, the WGS reaction follows a slope of 2; the oxygen transport is a vector that ends at the coordinates (O/C=2, H/C=0); and steam reforming reactions drive the represented cases towards higher H/C rations. This allows differentiation between steam reactions and oxygen transport. This is in contrast to other approaches used to assess gas conversion, e.g., based on steam consumption [103], which would aggregate the effects of the oxygen transport and steam reactions.

Tar groups are used according to the number of rings that they contain, as shown in Table 9. Peaks that correspond to species for which the instrument is not calibrated are lumped in the group SPA-Unknowns, and they account for 2-20% of the total mass detected in the SPA samples, depending on the case. When necessary, branched species and condensed rings are grouped separately to assess the levels of dealkylation reactions. Oxygen-containing species are treated separately, as they are expected to be rather sensitive to the operating temperature. Phenol is used as a representative oxygenated aromatic species owing to its abundance in the phenolic group. PAHs with four or more rings are used as an indicator of the extent of tar growth. In addition, naphthalene is used as reference tar species due to its abundance in the raw gas produced in commercial gasifiers (*cf.* Table 3), and because its concentration is reported for most units, which facilitates comparisons of the tar levels in different gasifiers.

The results derived from the HTR are treated in a manner similar to those of the permanent gas composition, i.e., calculated as the average of 10–20 chromatograms, and error bars show the standard deviation due to fluctuations of the process. Mass balance calculations are carried out based on the average values given by the different measurements, and the error bars account for the propagation of the standard deviation of the measurement.

Table 9. Groups of condensable species applied in this work for the carbon balance calculations. SPA refers to Solid Phase Adsorption.

	Group	Species included
SPA-measurable tar	Benzene:	benzene
	1-ring:	toluene, o/p-xylene, styrene, methyl-styrene
	Naphthalene:	naphthalene
	2-rings:	indene, 1,2-dihydronaphthalene, 1-methylnaphthalene, 2-methylnaphtalene, biphenyl
	>3-rings:	acenaphthylene, acenaphthene, fluorene, phenanthrene, anthracene, xanthene
	≥4-rings:	fluoranthene, pyrene, chrysene
	Phenols:	phenol, o/p-cresol, 1-naphtol, 2-naphtol
	Furans:	benzofuran, dibenzofuran
	SPA-Unknowns	Species that the instrument is not calibrated for but peaks are found in the chromatograms
Unidentified Condensable Species	UCS:	Other condensable hydrocarbons

The experimental method to estimate the extent of volatiles-bed contacts in **Paper I** is based on a tracer reaction between the volatiles and the bed material particles. The reaction used is the fast oxidation of volatile species by the oxygen carrier ilmenite. The fraction of volatiles in contact with the bed (X_{vol}) is estimated as the stoichiometric ratio of oxygen consumed by the volatiles, according to Equation 2. The oxygen consumed by the volatiles is calculated as the difference between the total oxygen consumed by the fuel ($\Delta\dot{m}_{O,total}$) and the oxygen consumed by the gasification products ($\Delta\dot{m}_{O,gasif\ products}$). Here, $\dot{m}_F$ denotes the fuel flow, and $\Omega_{S,j}$ is the stoichiometric oxygen for complete oxidation of the char ($j=char$) and the fuel ($j=F$). This expression assumes that all the H$_2$ and CO produced from the steam gasification of char is oxidized by the ilmenite bed. $\dot{m}_{O,j}$ and $\dot{m}_{H,j}$ are the yields of oxygen and hydrogen, respectively. M_w refers to the atomic mass.

$$X_{vol} = \frac{\Delta\dot{m}_{O,total} - \Delta\dot{m}_{O,gasif\ prod}}{\dot{m}_F \cdot \Omega_{S,F} - \dot{m}_{char} \cdot \Omega_{S,Char}} \qquad \text{Equation 2a}$$

$$\Delta\dot{m}_{O,total} = \left(\dot{m}_{O,HTR} - Y_{O,fuel}\right) + \left(\dot{m}_{H,fuel} - Y_{H,HTR}\right) \cdot \frac{M_{w,O}}{2 \cdot M_{w,H}} \qquad \text{Equation 2b}$$

$$\Delta\dot{m}_{O,gasif\ products} = \dot{m}_{char} \cdot X_c \cdot \Omega_{S,Char} \qquad \text{Equation 2c}$$

Char conversion (X_c) is estimated indirectly from the carbon balance according to Equation 3. Here, $\dot{m}_{char}$ refers to the yield of char and char composition and the values are assumed from a previous publication [104] in which relevant pyrolysis experiments with wood pellets in a fluidized bed are reported. $\dot{m}_{c,fuel}$ refers to the carbon content of the fuel according to the ultimate analysis, and $\dot{m}_{c,HTR}$ is the total carbon in the hot raw gas, as quantified with the HTR.

$$X_c = \frac{\dot{m}_{char} - (\dot{m}_{c,fuel} - \dot{m}_{c,HTR})}{\dot{m}_{char}} \cdot 100 \qquad \text{Equation 3}$$

The molar yield of carbon in the form of unidentified condensable species ($n_{c,UCS}$) is estimated from the carbon balance according to Equation 4.

$$n_{c,UCS} = n_{c,HTR} - n_{c,PG} - n_{c,SPA} \qquad \text{Equation 4}$$

The carbon in the SPA-measurable tar ($n_{c,SPA}$) accounts for the carbon in the 28 aromatic tar species listed in Table 9, and an estimate of the carbon in the group SPA-Unknowns. The latter is calculated assuming that the species corresponding to the unknown peaks have a similar molecular weight and carbon content as the next known specie in the chromatogram.

Validation tests for the combination of measurements were carried out, whereby the total carbon in the raw gas was quantified using two alternative approaches: (1) a combination of the SPA and permanent gas measurements; and (2) a measurement of the total carbon using the HTR. The tests were conducted under conditions in which the UCS fraction is negligible, i.e., at 820°C and with active bed materials [105]. Therefore, the SPA and permanent gas measurements should be sufficient to characterize the complete raw gas composition. Examples of the validation tests are shown in Figure 20, where the combination of SPA and permanent gas measurements covered 100±2% (shadowed area in the figure) of the carbon in the raw gas. The 2%-cut is indicative, and it corresponds to the typical standard deviation of the HTR measurement over a stable period.
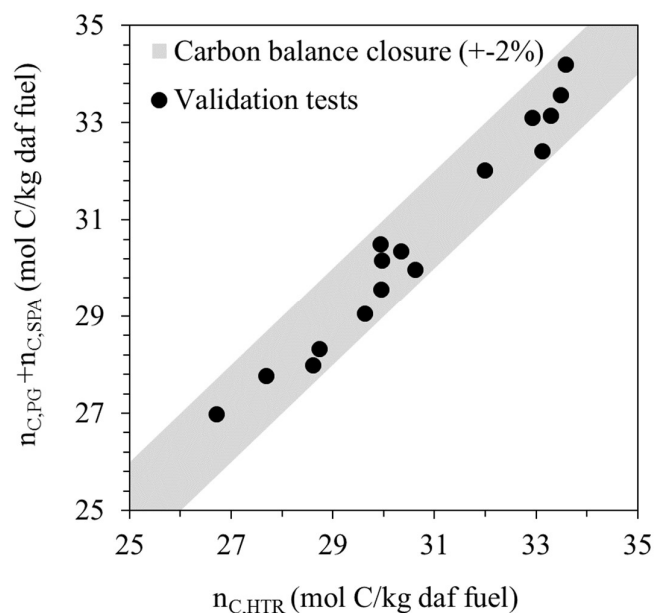
Figure 20. Validation of the quantification methods applied to characterize the raw gas composition. The total carbon in the raw gas was determined simultaneously using two different methods: a combination of SPA ($n_{C,SPA}$) and permanent gas ($n_{C,PG}$) measurements; and measurement of the total carbon in the raw gas in a HTR ($n_{C,HTR}$). UCS, unidentified condensable species.

Accurate quantification of the BTX species (benzene, toluene, xylenes) with the more efficient Supelclean ENVI-Carb/NH2 SPE columns improved the closure of the carbon balance by up to 5 percentage points depending on the operating conditions. BTX was found to account for 35%–70% of the carbon in the aromatic fraction measured by the SPA method.

5 - Results and discussion

Extent of volatiles-bed contacts. The estimated fractions of volatiles in contact with the bed material is presented in Figure 21, as well as their relations to the fluidization velocity. The estimates are conservative as the assumption is made that the kinetics of volatiles oxidation by ilmenite is rapid for all volatile species. The figure contains several repeat series, whereby the fluidization velocity was varied under different conditions, i.e., increasing the flow of fluidization steam while keeping the fuel flow constant, as well as simultaneous increases of the steam and fuel flows to maintain the steam-to-fuel ratio at a similar level. The fluctuations of the process result in a standard deviation for the calculated values of 3% (abs) or 10% (rel). At lower fluidization levels, the standard deviation was greater, which is probably related to the fluidization becoming more unstable as the flow of fluidization steam decreases.
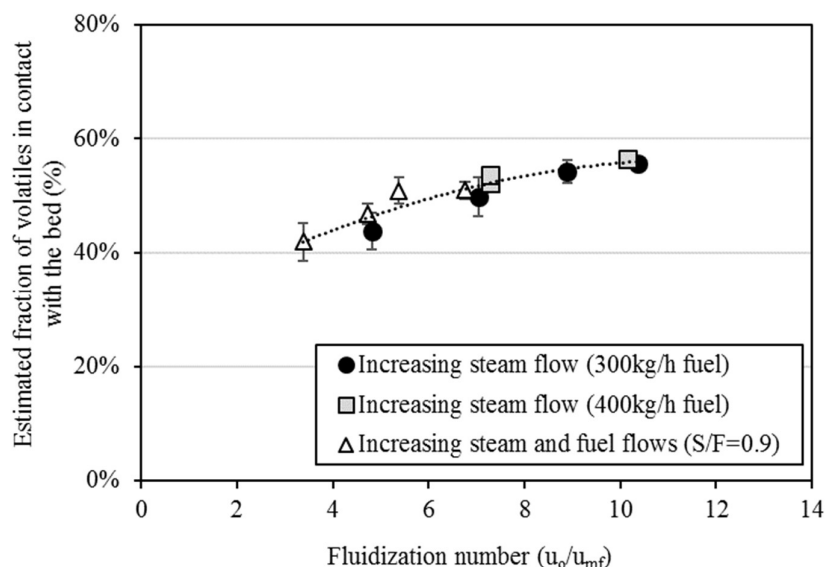

Figure 21. Conservative estimation of the fraction of volatiles ($X_{vol-bed}$) in contact with the bed material as a function of the fluidization number (u_o/u_{mf}). Three experimental series are included in the figure, whereby fluidization velocity was increased under different operating conditions, as indicated in the legend. S/F refers to the steam-to-fuel ratio. Shown are the averaged values over a stable measurement series and the corresponding standard deviation (if sufficiently large to be visible at reproduction scale).

At the lowest fluidization velocity tested, the fraction of volatiles in contact with the bed (X_{vol}) is roughly 40%, and it increases slightly with increasing fluidization velocity. The estimated level of contacts is surprisingly high considering: (i) the simple reactor design used in the

present work; and (ii) the tendency of the biomass particles to segregate. The results indicate that a fair degree of gas-solids contacts is attained through the mixing induced by the freely bubbling bed, provided that the bed is well-fluidized. In the present investigation, the bed is considered to be well-fluidized at fluidization numbers (u_o/u_{mf}) above 5-6.

The influence of fluidization velocity on the yield of tar that corresponds to the application of the tested bed materials is summarized in Figure 22. The yield of naphthalene is chosen because it can be accurately quantified with the two types of SPA-columns applied in the different measurements shown in the figure.
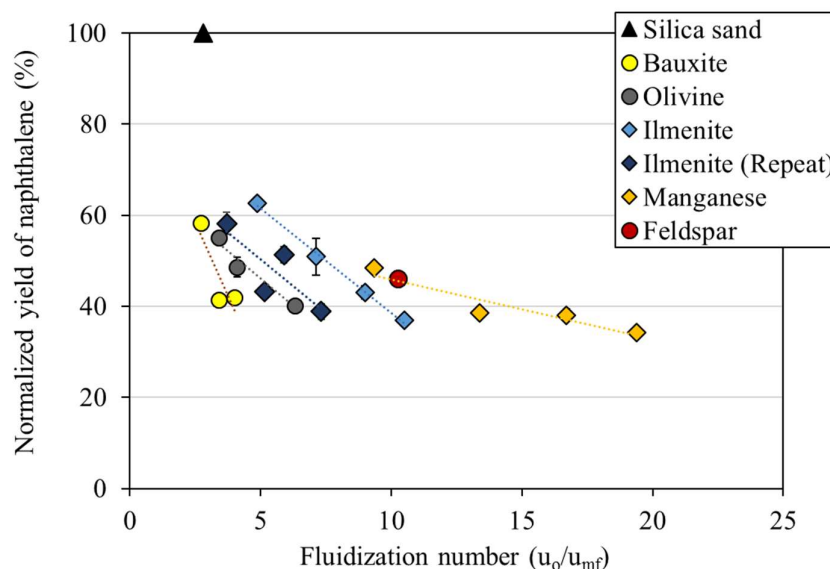

Figure 22. Normalized yields of naphthalene derived from applications of the different bed materials in the Chalmers gasifier and at different fluidization velocities. The naphthalene yield is normalized to a reference case with silica-sand, which represents 100%. Shown are the averaged values over a stable measurement series and the corresponding standard deviation (if sufficiently large to be visible at reproduction scale).

A higher fluidization number results in a steady decrease in the amount of naphthalene, while the slopes become flatter in the higher range of u_o/u_{mf} values. This trend is in good agreement with the relationship between the volatile-bed contacts and fluidization velocity shown in Figure 21, which indicates that part of the tar reduction may be attributed to the increasing volatiles-bed contacts. Note that the differences in the naphthalene yield among the experimental series are larger than the differences caused by a change in fluidization within each series, which shows that effects other than the extent of gas-solids contacts are influential, e.g., the activity of the bed.

Mapping of the main effects induced by the bed material on fuel conversion. The compositions of the permanent gases derived from the application of the bed materials tested are summarized in Figure 23, shown as the H/C and O/C molar ratios [3]. The pyrolysis case corresponds to the pyrolysis test reported previously [38] using wood pellets in an N_2 atmosphere. Each series contains cases with various S/F ratios (0.75–1.00), with increasing S/F as one moves from left to right in the figure, whereas only one case with S/F=0.8 is shown for feldspar. The standard deviations of the calculated H/C and O/C ratios are <3% (rel); they are included in the figure but not discernible.
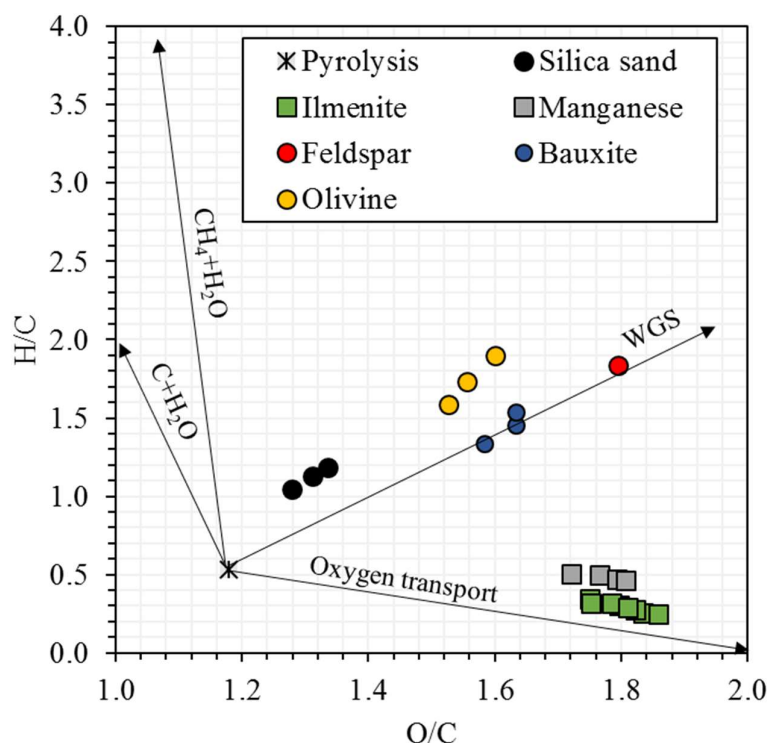

Figure 23. Molar H/C and O/C ratios of the syngas species (i.e., H_2, CO, and CO_2) corresponding to the operation of the Chalmers gasifier with different bed materials. For each series, the S/F ratio increases from left to right. The pyrolysis gas is from a pyrolysis experiment in an N_2 atmosphere. Shown are the averaged values over a stable measurement series and the corresponding standard deviation (if sufficiently large to be visible at reproduction scale).

The two functions of the bed material, i.e., catalysis and oxygen transport, are evident in the results. The catalytic materials and silica-sand show a similar response to an increase in S/F, which corresponds partially to the enhanced WGS, while the manganese and ilmenite yield a higher level of oxidation of volatiles. The catalytic activity of olivine seems to be superior to those of the other materials, while bauxite and feldspar have similar catalytic characteristics together with some degree of oxygen transport. The relative activity of silica-sand, olivine, bauxite, and the oxygen carriers can be expected from the original content of the bed material with regards to transition metals, in the order of: silica-sand<<olivine<bauxite<<manganese< ilmenite. However, the catalytic and oxygen transport capabilities of feldspar can only be attributed to its inherent content of alkali species and/or species added by feldspar-ash interactions.

Besides the reactions involving the permanent gases (WGS and oxidation of volatiles), all the active materials can decrease the yield of heavy tar by at least 40% compared to the case of silica-sand. This is shown in Figure 24, where the yields of naphthalene and heavier tar species are summarized for all materials tested under similar conditions of steam-to-fuel ratio and temperature. The cases selected correspond to materials of similar age, i.e., in their first week of operation, with the exception of the silica-sand, which is an old sand that is regenerated regularly. The influence of age will be discussed in the next section.
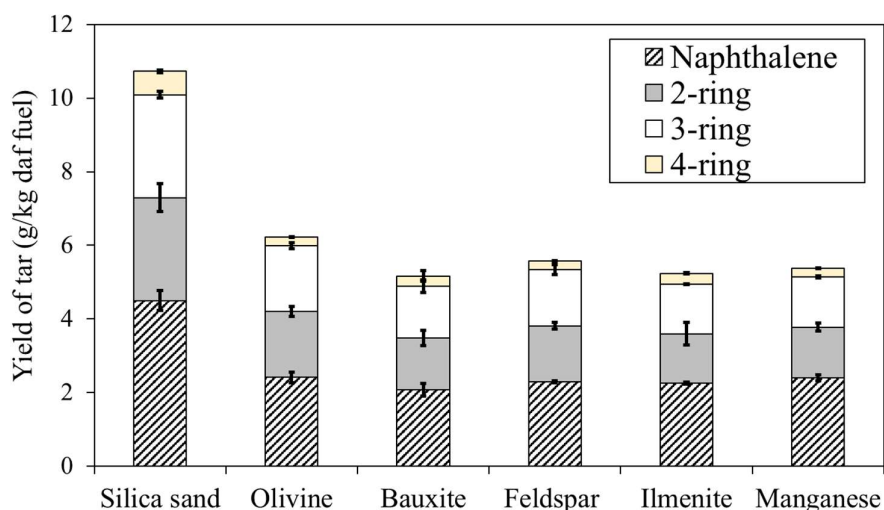

Figure 24. Yields of heavy tar derived through the use of various bed materials of similar age in the Chalmers gasifier operated under similar conditions: temperature, 810°–820°C; S/F=0.7-0.8; and wood pellets. The 3-ring tar group includes: acenaphthylene, acenaphthene, fluorene, xanthene, phenanthrene, and anthracene. The 4-ring tar group includes: fluoranthene, pyrene, and chrysene. The '2-ring' tar group includes: indene, dihydro-naphthalene, methylnaphthalenes, and biphenyl. Shown are the average values for four repetitions, and the corresponding standard deviation (if sufficiently large to be visible at reproduction scale).

The results show that oxygen-carrying capability is not essential for decreasing the tar yields in gasifiers. High-level oxygen transport mainly enriches the product gas with CO_2 and water due to the rapid oxidation of H_2 and CO, as observed with manganese and ilmenite in Figure 23. Similar yields of tar can be achieved regardless of the oxygen-carrying capacity of the bed.

Changes to the bed material properties due to ash accumulation. Throughout the work for this thesis it has been obvious that the catalytic and oxygen transport activities of the bed material are drastically altered over the operating time of the gasifier. Examples of the evolution of the yield of naphthalene as a function of accumulated operating time are shown in Figure 25 for experiments that started with beds of fresh feldspar and olivine, respectively. The cases labeled as 'ageing' correspond to activation of the material without additives, while the 'Olivine-S-K addition' case corresponds to an olivine that has been activated with the in-bed addition of K and S on the first day of operation. Each series presented in the figure contains data from two repeat experiments, which were carried out in different years.
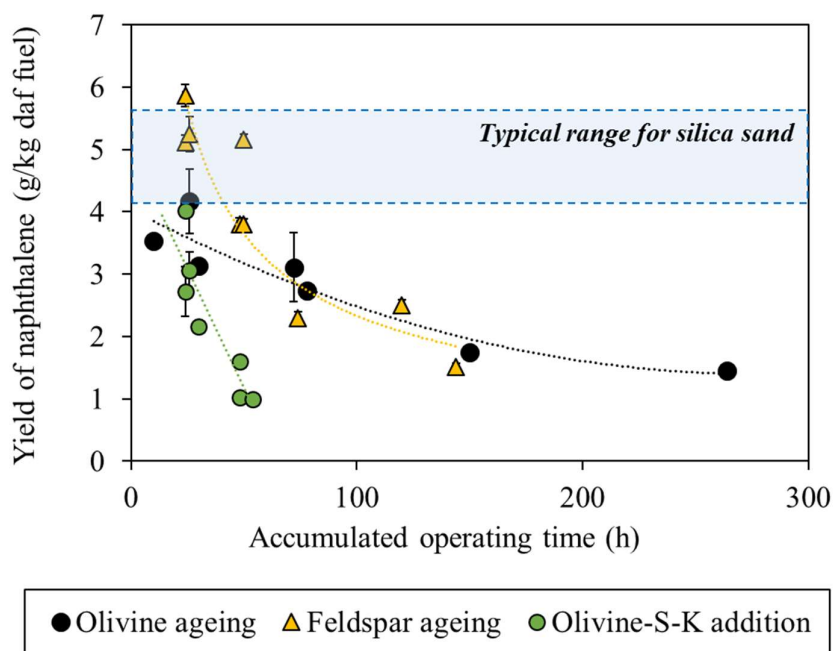

Figure 25. Yields of naphthalene as a function of operating time from start-ups with fresh olivine and feldspar, respectively. Olivine and feldspar ageing series corresponds to the activation of the materials due to the exposure to biomass ash from the fuel, exclusively. Olivine S-K addition, corresponds to a triggered activation by the in-bed addition of K_2CO_3 and elemental S on the first day of operation. Each series contains data from two repetitions. Shown are the averaged values over a stable measurement series and the corresponding standard deviation (if sufficiently large to be visible at reproduction scale).

The overall trend of the activation is rather reproducible, with larger variations among the repeat experiments at the early stage of activation, i.e., <50 hours of operation. The variations during the early activation stage can be partially attributed to differences in the initial state of the boiler, as well as to the higher sensitivity of the bed to the ash input before the ash coat has developed. In the two repeat experiments with addition of K and S to the olivine bed, the activation process was accelerated. In <50 hours (200 kg of cumulative fuel ash input), the olivine bed had a higher catalytic activity than olivine that was aged for more than 200 hours (>800 kg of cumulative fuel ash input) and that was without additives.

The dominant role of the biomass-ash elements in the catalytic properties of the bed inventory was further confirmed by recirculating into the gasifier the ash-rich stream separated by the flue gas cyclone. The results are summarized in Figure 26 and Figure 27 for olivine and feldspar, respectively. The ratio of circulating bed material to ash at the inlet of the gasifier was 13 tons bed/h to 200 kg ash/h, i.e., 1.5% ash.
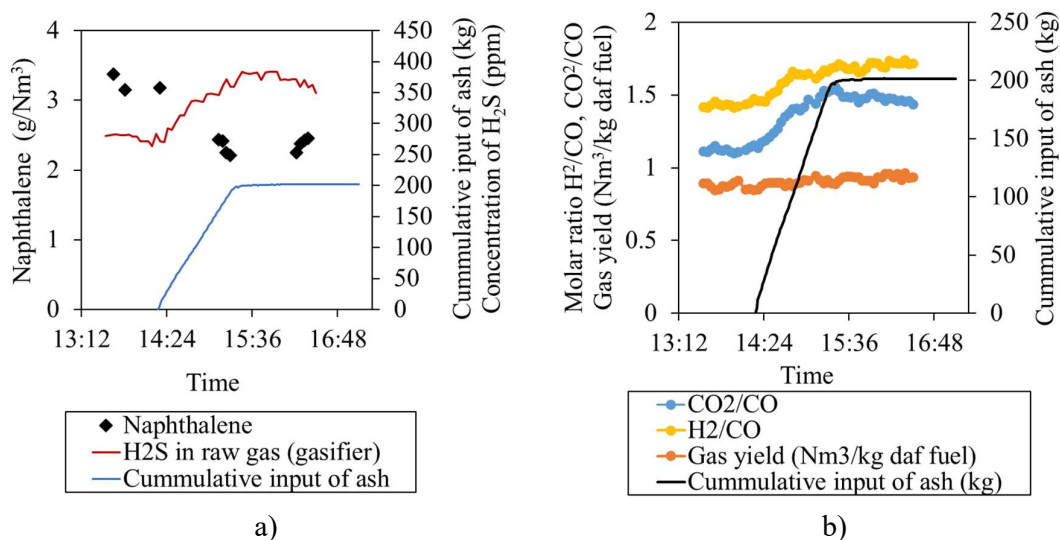

a)   b)

Figure 26. Recirculation of fly ash into the Chalmers gasifier equipped with a bed of olivine. Transient measurements of: a) the concentrations of naphthalene in the raw gas based on SPA samples and of H_2S based on μ-GC measurements; and b)) the molar ratios of H_2/CO and CO_2/CO, and the yield of raw gas based on He-tracing and μ-GC measurements.

a)   b)
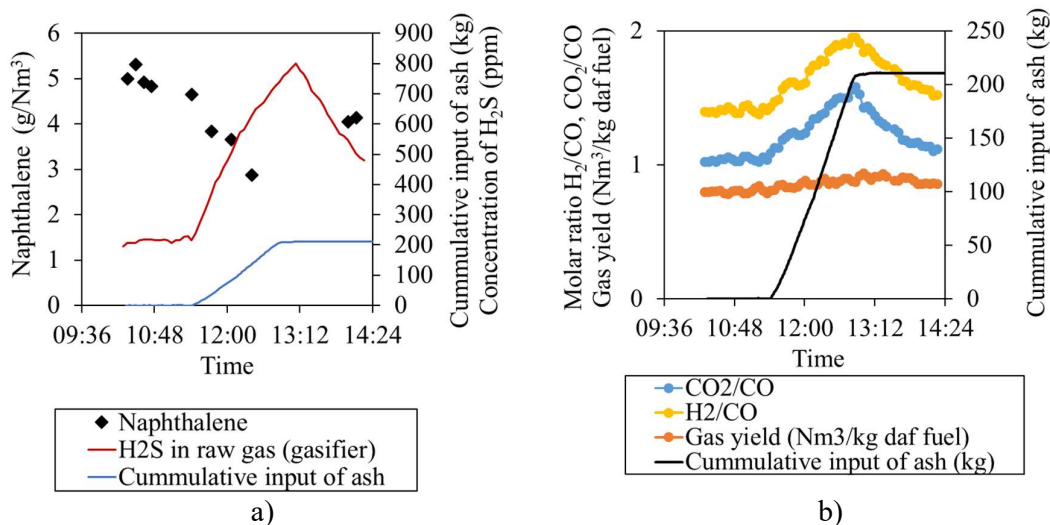
Figure 27. Recirculation of fly ash into the Chalmers gasifier equipped with a bed of feldspar. Transient measurements of: a) the concentrations of naphthalene in the raw gas based on SPA samples and of the concentration of H_2S based on μm-GC measurements; and b) the molar ratios of H_2/CO and CO_2/CO, and the yield of raw gas based on He-tracing and μ-GC measurements.

The presence of ash in the system clearly enhances the WGS and reduces the tar yields for both olivine and feldspar. This is deduced from the simultaneous increases in the H_2/CO and CO_2/CO ratios, as well as the reduction in the levels of tar as the ashes are introduced. This also shows that a substantial fraction of the catalytic activity of the bed can be attributed to the ash species accumulated in the system, regardless of the original concentrations of transition metals in the material. In this case, the concentrations of Fe in the olivine and feldspar differ by roughly two orders of magnitude, yet both materials develop significant catalytic activities after exposure to biomass ash, as shown in Figure 25.

A remarkable difference between feldspar and olivine ageing is that feldspar developed different properties during activation (**Paper IV**). In two repeat experiments, untreated feldspar material acquired high catalytic activity towards tar and WGS during ageing. However, in one of these repeat experiments, further ageing resulted in a marked oxygen transport capacity, as shown in Figure 28. The standard deviation of the *catalytic* and *untreated cases* is somewhat larger than that of the *oxygen transport* case, as the values shown are the average of the two repeat activation experiments starting from a batch of untreated feldspar. In contrast, for the *oxygen transport case*, the error bars represent the standard deviation during a stable measurement, as a repeat experiment was not possible.
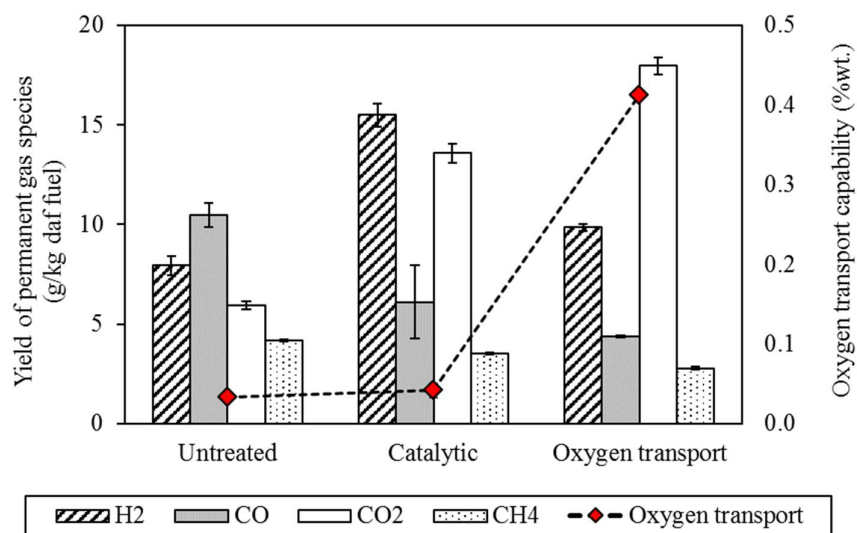

Figure 28. Permanent gas yields measured in the Chalmers gasifier equipped with a bed of untreated feldspar, catalytic (ash-coated) feldspar and feldspar with oxygen-transport properties. The following gasifier conditions were used: wood pellets; 820°C; and S/F=0.8. The secondary axis shows the oxygen-transport capabilities of the three samples, which were quantified in a laboratory test carried out with a 50:50 mixture of H_2 and CO, at 820°C.

Based on SEM-EDS analysis of the oxygen-carrying feldspar, the compound that expresses the oxygen-carrying properties most likely contains S, Mn and/or Fe. The reason for pinpointing these three elements is that they were present (in concentrations above the detection limits) when the oxygen-carrying capability was observed, but not earlier. Fe and Mn are known carriers of oxygen and therefore, they likely contribute to the oxygen-transport capability. To

test whether S was also involved in the oxygen transport, elemental S was added to the bed (boiler side) while monitoring the gas composition. The results are shown in Figure 29.

a)   b)
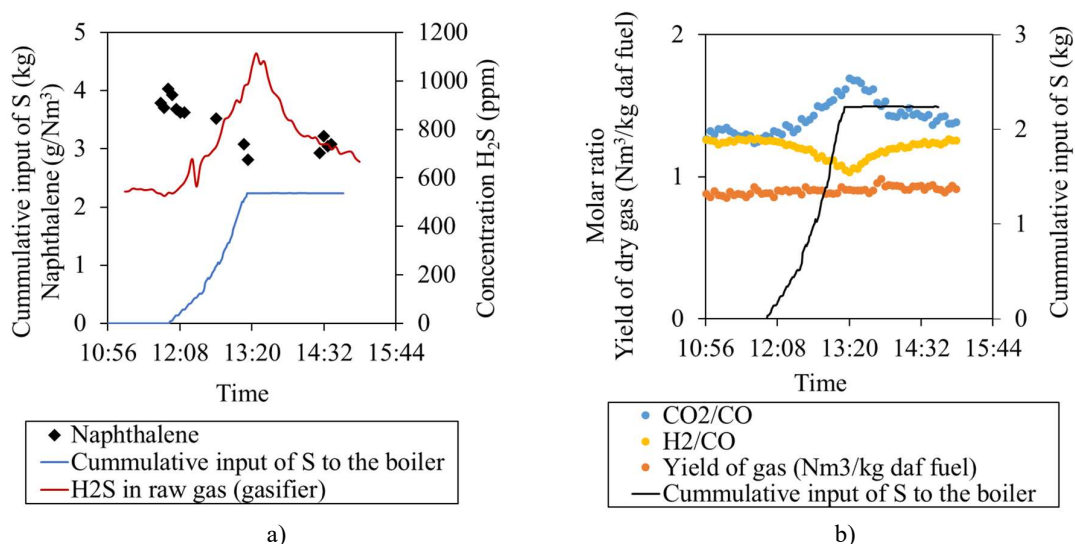
Figure 29. Influence of sulphur addition to a bed inventory of 3 tonnes of feldspar. Transient measurements of: a) the transport of sulphur from the boiler to the gasifier by the bed material; and b) the net oxygen transport effect on the permanent gases.

The oxygen-carrying ability of the added sulfur was evidenced by an increase in the CO_2/CO ratio concomitant with a decrease in the H_2/CO ratio. The increase in the amount of H_2S in the raw gas composition (Figure 29a) during the addition shows the capability of feldspar to transport S, which is in line with the experience with olivine.

Influence of bed material properties on char gasification rate. The application of different bed materials in the Chalmers gasifier resulted in different degrees of char conversion; some of the char results are summarized in Figure 30. The char conversion rate is indirectly estimated by the carbon balance, and it is based on measurement of the total carbon in the hot gas ($n_{c,HTR}$), as described in Section 4.5. The total carbon measured by the HTR is relatively stable, despite the fluctuations in the process, and it has a relative standard deviation of <5% in most cases. However, in the calculation of the char conversion (Equation 3), this uncertainty propagates, yielding standard deviations of the char conversion estimate in the range of 5%–15% (abs).
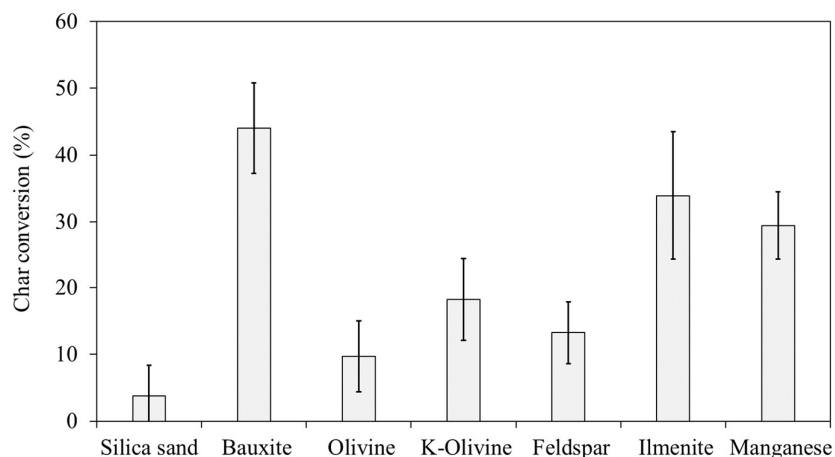

Figure 30. Estimated char conversion rates from the application of various bed materials in the Chalmers gasifier. The operating conditions were: steam gasification of wood pellets; bed temperature of 820°C; and S/F=0.8. K-olivine refers to an olivine that has been activated by the addition of S. Shown are the average values for stable measurement over 30-60 minutes, and the corresponding standard deviation.

The range of char conversion values obtained was 0%–50%, and higher conversion rates are typically attained with active bed materials compared to a reference case with silica-sand. In the case of the oxygen carrier ilmenite, the enhanced kinetics appear to be the result of less inhibition by volatile species, as proposed in the literature [47, 106]. However, for the catalytic materials, the oxygen-carrying capability is modest compared to that of ilmenite (Figure 23), and oxygen transport cannot on its own explain the high rate of char conversion. It was proposed that the transfer of catalytic species from the bed to the char plays a role in DFB gasifiers. This hypothesis was tested in the laboratory setting using wood char and olivine that was activated through in-bed addition of K and S. The analysis of the cross-section of the partially gasified char is shown in Figure 31. The figure also includes a reference test with wood char and untreated olivine.
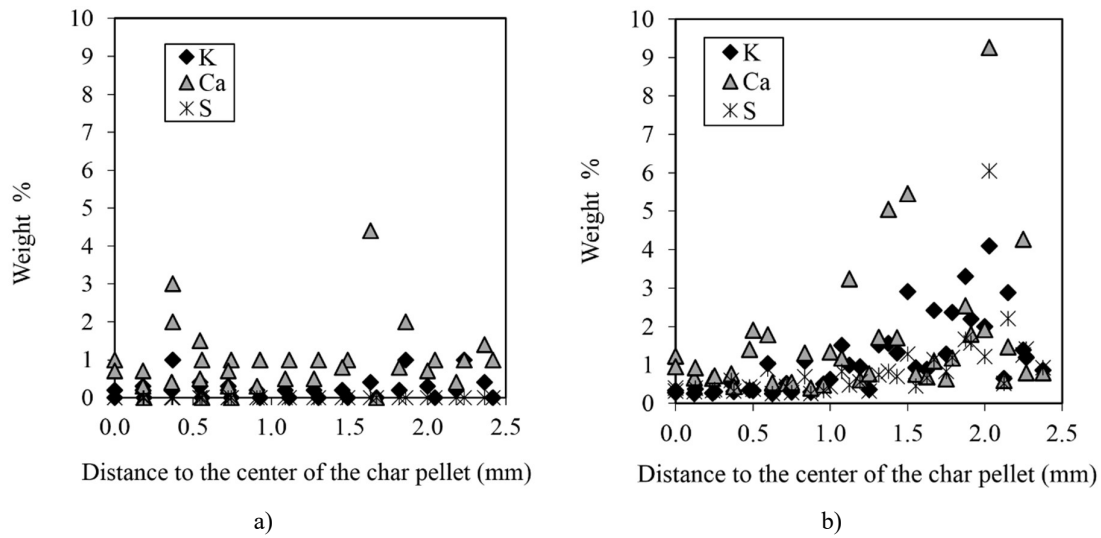
Figure 31. Concentrations of K, Ca, and S across the cross-section of a partially gasified wood char pellet (Xc=40%). Gasification in steam was conducted at 900°C in a bubbling bed of; a) fresh olivine; and b) ash-coated olivine.

The active olivine clearly transferred K and S to the char particles (Figure 31b), and this is in line with the activation method of the bed material. Regarding the Ca, the bed material analysis did not provide sufficient evidence that Ca particles can also be transferred from the bed to the char. A similar transfer of catalytic species is likely to occur when bauxite is used as the bed material, as its ability to enhance the char gasification rate cannot be explained by its oxygen-carrying capability. The laboratory tests carried out with the alkali-loaded olivine also showed that the ability of the olivine to catalyse the steam gasification reaction declines as the alkali content of the material is depleted. Therefore, a relationship between the alkali load of the bed material and catalytic activity is expected

The influence of oxygen transport on char conversion was investigated for ilmenite (strong oxygen carrier) and feldspar (moderate oxygen-carrying capability). The availability of oxygen carrier per unit fuel was changed by modifying the flows of bed material and fuel. The results for char conversion are shown in Figure 32. The wide spread of the data (average values) is partially due to the interplay of residence time and oxygen-carrier availability in the results. Nevertheless, some trends can be distinguished despite the relatively large uncertainty of the measurement. For instance, higher availability of oxygen carrier per unit fuel results in an increased rate of char gasification for ilmenite, whereas for the moderate oxygen carrier feldspar, the oxygen transport could not compensate for the shorter residence time induced by the increase in circulation rate.
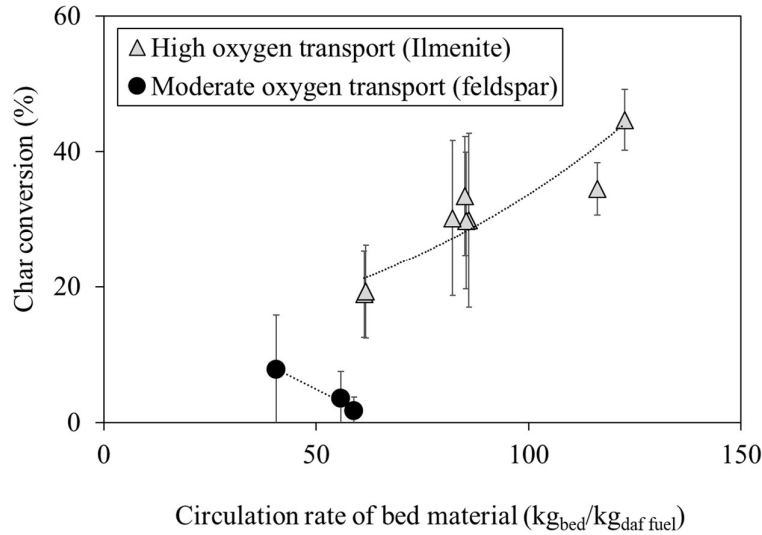
Figure 32. Estimated char conversion rate (%) as a function of the circulation rate for a strong and a moderate oxygen carrier, respectively. In the figure, an increasing circulation rate implies shorter residence time for the char in the reactor and higher oxygen transport per unit fuel. Shown are the average values over a 30-60 min measurement under stable conditions, and the corresponding standard deviation.

It can be inferred that the char gasification rate is partially controlled by the availability of active species carried by the bed material, which can be in the form of: (1) releasable alkali; and/or (2) reducible oxides in the case of oxygen carriers. The availability of releasable alkali that can catalyze char gasification can be enhanced by additives, as confirmed by the case of olivine activated with K and S. Further enhancement of the char gasification rate by means of oxygen transport should not be expected in DFB gasifiers, in which oxygen transport is moderate.

Control of formation of aromatic tar. In this work, the condensable species have been divided into the SPA-identified fraction and other unidentified condensable species (UCS) species (Table 9). Figure 33 shows the relationship between the operating temperature and the yields of UCS and SPA (mol C/kg daf fuel), for a low-activity bed (silica-sand) and for activated olivine. Repeat experiments (from the same and different experimental campaigns) are included in the figure to visualize the spread of the data. The trend-lines are linear fits of the corresponding series of measurements.

The SPA-results showed good reproducibility, with the repeat values remaining within a range of $\pm$ 0.3 mol C/kg daf fuel from the average, i.e. 20% (rel) standard deviation. In contrast, the reproducibility of the UCS estimate was poorer, particularly for the active olivine cases, for which the UCS results are spread in an area of $\pm$ 1mol C/kg daf fuel from the average. Generally, it can be noticed that there is a region of high uncertainty of the UCS measurement for values below 1mol C/kg daf fuel. This is partially explained by the small yield of UCS combined with the accumulation of uncertainties of the three parallel measurements (recall Equation 4). Accordingly, the spread of the UCS results for silica sand is significantly lower, as the yield of UCS rapidly increases at lower temperatures and leaves the high uncertainty region. Note that

the high uncertainty region contains negative values that do not have a physical meaning, but they contribute to the statistical significance of the trends observed.
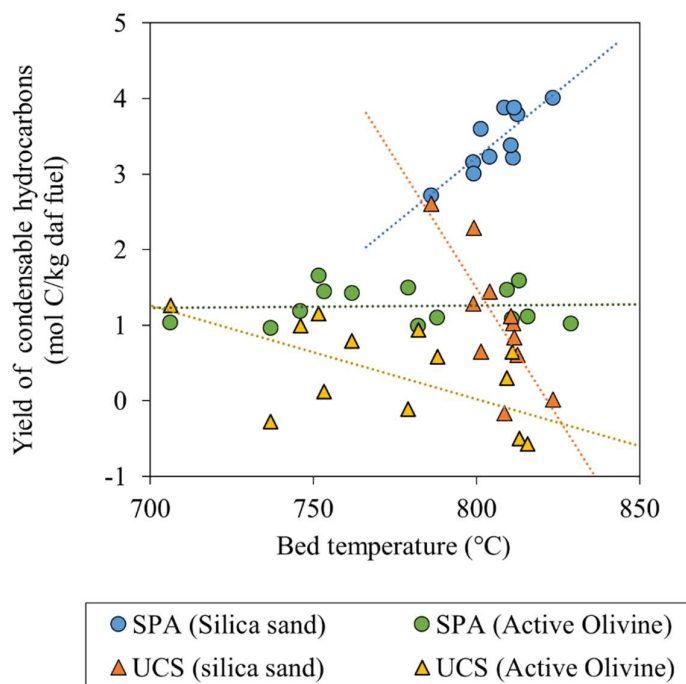

Figure 33. Temperature dependence of the yields of SPA tar and UCS in units of mol C/kg daf fuel, derived from the use of silica-sand and olivine in the Chalmers gasifier. Each case is the average of a 30–60 min stable measurement. Trend-lines are linear fits of the data.

On average, the yield of UCS species decreases with temperature for both materials. With silica-sand, 50% of the converted UCS (due to an increase in temperature) becomes SPA-measurable tar, whereas with active olivine the yield of SPA tar (in units of mol C/kg daf fuel) remains rather stable. These trends show that the UCS fraction is thermally unstable and it is a source of aromatics in the absence of catalyst. The results support the notion that the UCS fraction is rich in primary tar, which are earlier precursors to the formation of aromatic species measured by the SPA method. The presence of primary tar in the raw gas accords with the relatively low temperature applied in the Chalmers gasifier.

The active olivine is clearly active towards the conversion of the UCS species. With active olivine the conversion of UCS yields permanent gases instead of SPA tar. On average, 60% reduction of the SPA is achieved by olivine as compared to silica sand at 780°C. According to the slopes in Figure 33, roughly 40 percentage points of the tar reduction can be attributed to the prevention of tar formation, whereas 20% of the reduction can be attributed to the catalytic reforming of aromatic tar. The latter has been proven by Kubba et al. [91, 92] with ash-layered olivine and toluene and indene. Therefore, the ability of active olivine to decrease the yield of tar can be attributed in part to the catalytic conversion of primary tar species into permanent gases, thereby preventing their further aromatization.

46

It is noteworthy that, with active olivine, the yield of UCS species approaches zero at temperatures at which the UCS predominate in a silica-sand bed, e.g., below 800°C. This means that thermal cracking cannot explain the complete conversion of UCS at these temperatures. The heterogeneous catalysis by olivine can difficulty explain such high conversion of UCS provided the limitations of the gas-solid contacts discussed above. A catalytic mechanism that enables full conversion of UCS species is needed to explain the results. This is possible if homogeneous interactions of the ash layer and the nascent tar are considered. For instance, the alkali released from the olivine bed could contribute to the decomposition of cellulose-derived vapors, which is in line with previously reported findings [96]. The results presented here are not sufficient to elucidate the homogeneous interaction that is involved. Therefore, it can only be concluded that gas-phase interactions of nascent volatiles and the bed material are relevant to DFB gasifiers that have (ash-coated) in-bed catalysts.

Under the conditions tested, increasing the operating temperature did not influence significantly the tar yield (in units of molC/kg daf fuel) when active olivine was applied as the bed material. Instead, the operating temperature was found to determine the tar composition, as shown in Figure 34. The ratio of phenol to naphthalene is here used as an indicator of the maturity of the tar composition, as these are the most abundant phenolic and condensed polyaromatic species, respectively. Increasing the bed temperature from 750°C to 850°C decreases this ratio from approximately 2.3 to close to zero. Note that the correlation in Figure 34 is independent of the bed material used, as it rather relates to the thermal stabilities of the phenol and naphthalene molecules.
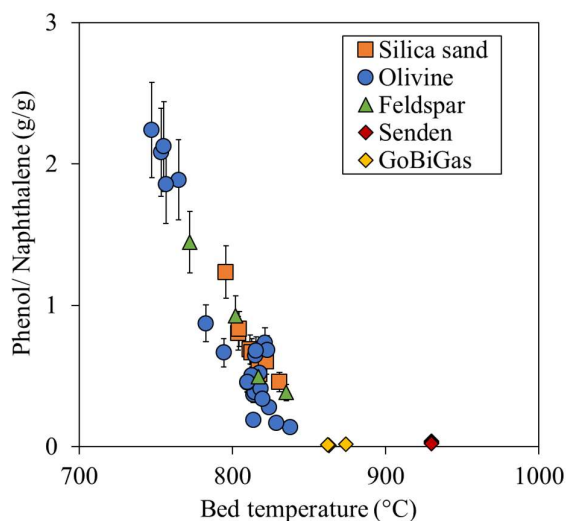
Figure 34. Ratios of phenol to naphthalene as a function of the operating temperature for cases with silica-sand, olivine, and feldspar as the bed materials in the Chalmers gasifier, as well as for the GoBiGas and Senden gasifiers operating with olivine. Shown are the average values over a stable measurement. For the Chalmers data, the error bars indicate the standard deviation when it is sufficiently large to be visible at reproduction scale.

The operating temperature partly explains the differences in tar composition derived in the Chalmers and in the Senden and GoBiGas gasifiers, in which the temperature is typically

>850°C. For instance, the two commercial gasifiers produce a tar that is essentially phenol-free and rich in naphthalene, i.e., 3-6-fold the values obtained in the Chalmers gasifier. In addition, the branched aromatics are a minor fraction in the tar produced at the GoBiGas plant, whereas the branched species toluene is more abundant than naphthalene in the raw gas from the Chalmers gasifier. This is also in accordance with differences in the operating temperature, as exemplified in Figure 35 for an active bed of olivine at 700°C and 830°C, respectively. Overall, the higher bed temperature promotes the secondary reactions of tar and reduces the number of species in the tar, enriching the tar fraction for benzene, naphthalene, and other non-branched aromatics
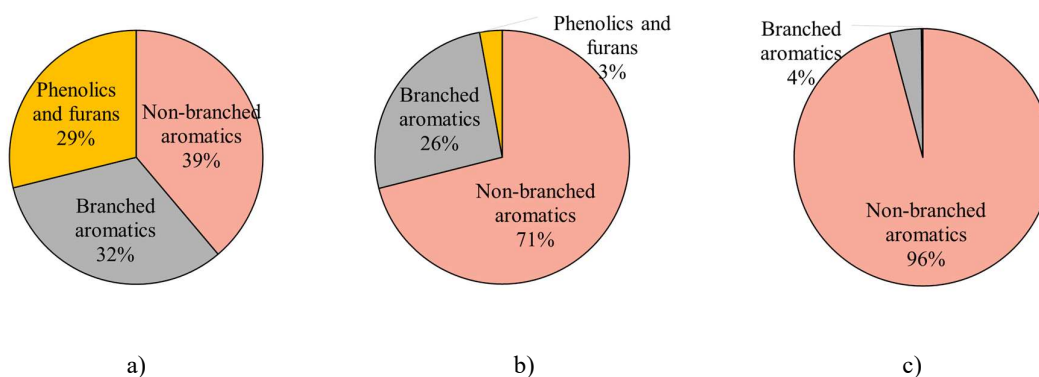
Figure 35. Shares of tar species in the raw gas produced in the Chalmers gasifier operating with active olivine at a) 700°C; and b) 830°C; and c) in the GoBiGas gasifier operating with olivine at 870°C [33]. Tar measured by the SPA method (including BTX), and sorted into branched, non-branched and oxygen containing compounds.

Furthermore, some contribution of the freeboard to the secondary reactions of tar is expected in the large gasifiers, as the freeboard can be at temperatures above 800°C. This prolongs the residence time of the tar in a reactive environment in which dealkylation reactions can take place. In contrast, the secondary reactions in the freeboard are minimized in the Chalmers gasifier, as the raw gas temperature is in all cases below 800°C due to the relatively low bed temperatures investigated. It is, therefore, plausible that the hotter freeboard of the GoBiGas reactor also contributes to the reduction of the number of tar components shown in Figure 35.

5.1 Comparison of strategies to control the concentration of tar

An overview of the raw gas quality and yield for different operating conditions in the Chalmers gasifier is presented in Figure 36. Each bed material series includes cases with different operating conditions (S/F, fluidization velocity, temperature). The shadowed area encloses the cases with low catalytic activity, i.e., the silica-sand cases and the first days of operation with feldspar and olivine, when their activities are low.
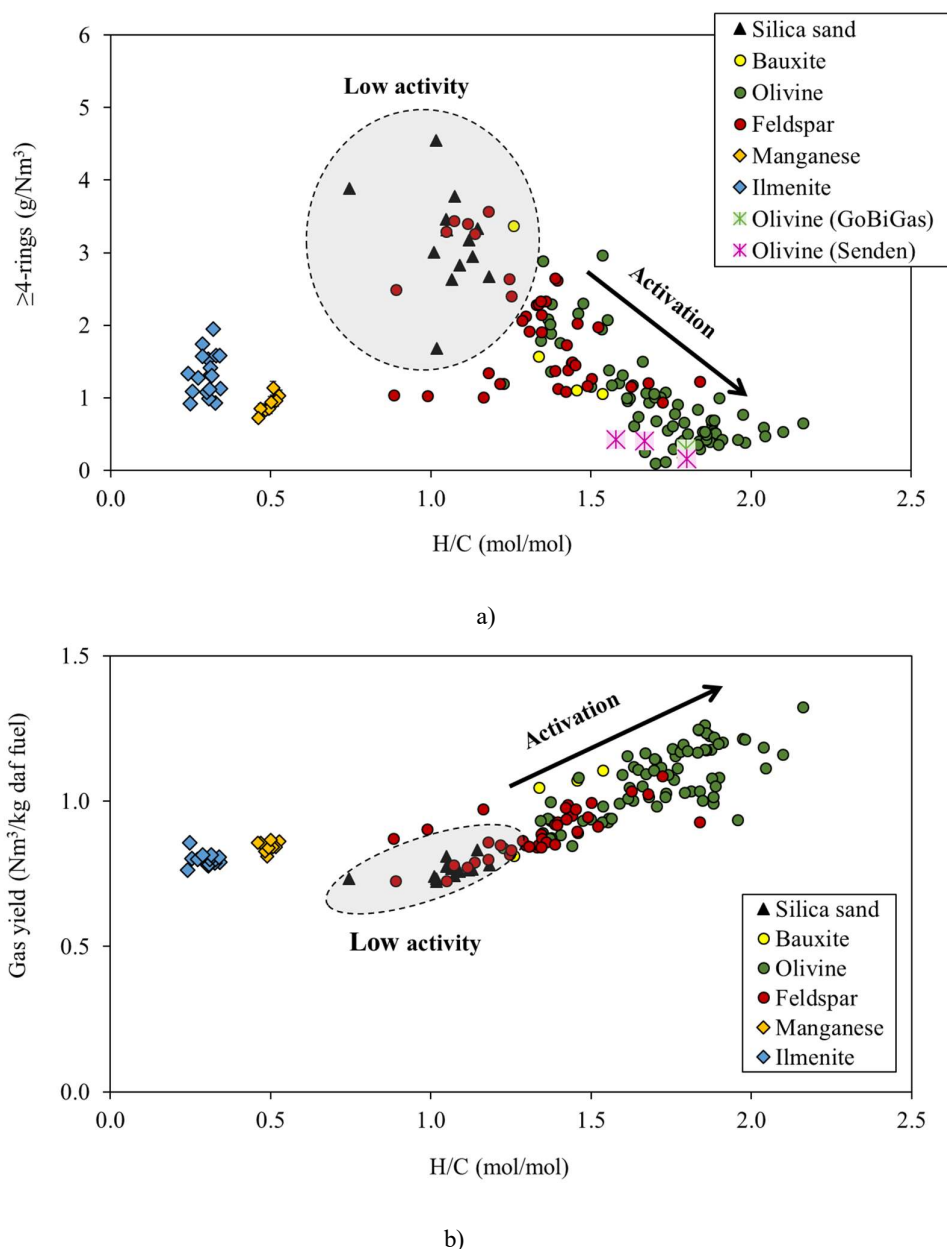

a)

b)

Figure 36. Overview of the raw gas quality and gas yield for different operating conditions (temperature, steam-to-fuel ratio, residence time) and different bed materials applied in the Chalmers gasifier. a) Concentrations of heavy tars ($\geq$ 4-rings) in relation to the H/C molar ratio; b) yields of dry raw gas in relation to the H/C molar ratio.

When applying non-active materials in the Chalmers gasifier (indicated as the low activity areas in the figures), the concentrations of heavy tars ($\geq$ 4-rings) vary within the wide range of 1.6–4.7 g/Nm^3 depending on the operating conditions. The lowest concentration is obtained at low temperature (i.e., 780C°). However, this occurs at the expense of carbon conversion and gas yield, as depicted in Figure 36b. Under the conditions tested, concentrations of heavy tars ($\geq$ 4-rings) of <1 g/Nm^3 with gas yields >1 Nm^3/kg daf fuel could only be achieved with active olivine, feldspar, and olivine. In those cases, the activation level achieved through exposure to active inorganic elements from the biomass ash or additives (shown by the arrow in Figure 36) resulted in the highest tar reduction, as compared to other investigated changes in the operating conditions, i.e., the steam-to-fuel ratio, temperature, and circulation rate.

For all the experimental cases included in the figure, the tar concentration exceeds the limits for synthesis applications, for combustion in gas engines and gas turbines, as well as for pipeline transport prior to compression, according to the data reported elsewhere [6] and summarized in Table 1. Therefore, additional secondary measures are required if the gas produced by biomass gasification in a DFB system is intended for applications other than direct combustion on-site.

5.2   Implications of the results for the operation and design of DBF gasifiers

The possibility to produce in the Chalmers gasifier a gas with tar concentration similar to those produced in the GoBiGas and Senden plants points to the fact that a simple gasifier design can yield high fuel conversion rates if the bed material has high catalytic activity. The design choices that are commonly considered to yield poor gas-solids contacts, e.g., over-bed fuel feeding [107] and simple shape [34], have been here shown to be capable of ensuring that roughly half of the volatiles come in contact with the bed material when the bed is well-fluidized. The results also support the idea that the combined effect of heterogeneous catalysis and homogeneous catalytic interactions contributes to the reduction of tar in a system with an excess of alkali with respect to free SiO_2, as in the cases of olivine and wood. Therefore, a complex shape of the freeboard that enhance gas-solids mixing, and in-bed fuel feeding can be avoided.

The results presented here support the proposition that activation of natural bed materials during biomass gasification is linked to the input of ash species with the fuel. It is shown that the artificial addition of inorganic compounds to the system accelerates this activation process. In the case of olivine, the combined addition of potassium and sulfur accelerates activation and confers on the olivine the ability to release catalytic potassium in the gas phase in the reactor. Therefore, it is recommended that commercial DFB gasifiers count with systems for the storage and introduction of additives, as well as equipment to store and reintroduce ash streams that are rich in catalytic species. These strategies are reasonable for bed materials that have weak tendencies to agglomerate due to the formation of low-melting-point silicates, e.g., materials with low contents of free SiO_2.

The experiences gained with olivine and feldspar in the Chalmers gasifier indicate that olivine is the more robust catalyst (i.e., has a more resilient catalytic activity). For instance, the tested

feldspar material developed either a marked catalytic activity or a marked oxygen transport capability depending on the development of the ash layer. In contrast, the activation of olivine resulted in a marked catalytic activity in all the repeat experiments. One hypothesis is that this is related to the Fe content of the olivine, which provides additional catalytic activity that is not dependent upon the presence of the ash layer. The results presented here are not sufficient to elucidate the catalytic species in ash-coated materials or the underlying processes that trigger the development of different properties, such as catalytic and oxygen-carrying properties. Detailed characterization of the bed material would help in this context, while generalizations and rankings of bed material activities should be carried out with care, since they strongly depend on the ash exposure history of the sample.

The present investigation shows that the effectiveness of in-bed catalysts in DFB biomass gasifiers in decreasing the tar yield can be attributed to the enhanced conversion of nascent tar into permanent gases, thereby preventing their subsequent maturation into aromatic species. This confirms the hypothesis that was first suggested by Corella and co-workers [99]. According to the results presented here, the catalytic actions of the ash-coated materials tested on nascent tar are relevant at temperatures below 800°C. This means that gasification with in-bed catalysts can be carried out at temperatures lower than the typical range of temperatures applied in commercial DFB gasifiers (850°–900°C), and without a penalty being imposed on the total yield of condensable species. The adjustment of temperature is rather a tool to control the composition of the resulting tar.

Furthermore, it is recommended that the use of oxygen carriers should be minimized in DFB gasifiers where the CO_2 should be removed from the raw gas stream. According to the results, the application of oxygen carriers in DFB gasifier results in a CO_2-enriched raw gas due to rapid oxidation of H_2 and CO. Significant benefits from oxygen carriers (compared to other natural materials) in terms of char conversion and tar reduction should not be expected in DFB gasifiers. For instance, the tar reduction ability of oxygen carriers is similar to that of other non-oxygen-carrying materials tested in this work, and the char gasification rate was not enhanced by oxygen transport at conditions relevant to gasification, i.e., $\phi < 1$.

This thesis has focused on the gasification of woody biomass, and it shows that operational strategies exist to overcome the major technical challenge of excessive tar formation in fluidized bed steam gasifiers. Economic aspects are likely to be a more serious hurdle to the application of the technology than the maturity of the technology itself. Flexibility of feedstocks and products can contribute to the economic feasibility of the gasification technology. However, the choice of feedstock is constrained by availability, price, and sustainability criteria. Woody biomass is, for instance, relevant to regions in which wood is an abundant and well-managed resource, and where the product price justifies the economic viability of the gasification plant. To contribute to a circular economy, residual streams can also be considered, e.g., forest and farming residues, and rubber/plastic-containing waste streams. The economic and resource aspects of gasification fall outside the scope of this thesis.

6 - Summary and conclusions

In this thesis, various strategies to control the yield of tar in dual fluidized bed (DFB) gasifiers have been investigated experimentally in a 2–4-MW$_{th}$ DFB gasifier. The yields of tar and permanent gas species, as well as the char conversion rate have been quantified for steam gasification of woody biomass under various operating conditions. The work has been exploratory, and it has covered a wide range of primary measures for tar control, the effectiveness levels of which have been compared to each other. The operating conditions investigated in this work are: fluidization velocity; active bed materials; steam-to-fuel ratio; circulation rate; and temperature. The main conclusions of this work are:

- A simple gasifier design with on-bed feeding should be considered a suitable design for large biomass gasifiers. Fluidization numbers of u_o/u_{mf}>5–6 ensure that roughly 50% of the volatiles are in contact with the bed material.

- Within the operating window explored in this thesis, the most effective measure to limit the production of tar in a DFB gasifier is optimization of the catalytic activity of the bed material applied.

- For a given bed material, its activity is primarily dictated by the properties of the ash layer formed, which in turn depend on the fuel ash composition and/or additives applied. In line with this, the properties of the bed material can be deliberately modified through the use of additives that become incorporated into the ash layer. In this work, combinations of S and K have shown to be good promotors of the catalytic activity of olivine.

- The ash-coated materials prevent the formation of aromatic species through the catalytic conversion of early tar precursors into carbon oxides and hydrogen. Additional inhibitory effects of tar polymerization and/or catalytic destruction of mature tar may also participate in this process. These mechanisms warrant further investigation.

- The ash layer on the bed material particles can catalyze the char gasification reaction. This occurs if K is hosted in the ash layer and is released and transferred to the char particles. This phenomenon has been demonstrated for ash-coated olivine.

7 - Recommendations for future research on gasification

The current knowledge on the mechanisms underlying the catalytic activities of ash-coated bed materials is incomplete. It is recommended that future research in the field of fluidized bed gasification should enhance fundamental understanding of:

- Ash-layer formation and its relation to catalysis and oxygen-transport capabilities. This would involve, for example, elucidation of the factor(s) that trigger the development of different properties of the same bed material. New knowledge in this area would help to predict the evolution of bed material properties in relation to the composition of the fuel applied.

- The mechanisms of tar formation and decomposition in the presence of ash-coated materials. This would involve clarification of the nature of the catalytic properties of the ash layer, e.g., homogeneous vs. heterogeneous catalysis, active species, and reactivities towards oxygenated compounds and different types of hydrocarbons.

These areas of research would contribute to generalizing the experience gained with woody biomass to any carbon-containing waste stream, which in turn would increase the versatility of the gasification process.

References

1. *Proposal for a DIRECTIVE OF THE EUROPEAN PARLIAMENT AND OF THE COUNCIL on the promotion of the use of energy from renewable sources* in *COM/2016/0767 final/2 - 2016/0382 (COD)*, E. Comission, Editor. 2016.
2. *Proposal for a DIRECTIVE OF THE EUROPEAN PARLIAMENT AND OF THE COUNCIL amending Directive 2003/87/EC to enhance cost-effective emission reductions and low-carbon investments*, in *COM/2015/0337 final - 2015/0148 (COD)*. 2015.
3. Larsson, A., *Fuel conversion in a dual fluidized bed gasifier*, in *Department of Energy and Environment*. 2014, Chalmers University of Technology: Gothenburg, Sweden.
4. Lundberg, L., et al., *Influence of surrounding conditions and fuel size on the gasification rate of biomass char in a fluidized bed.* Fuel Processing Technology, 2016. **144**: p. 323-333.
5. Milne, T.A., N. Abatzoglou, and R.J. Evans, *Biomass gasifier" tars": Their nature, formation, and conversion*. Vol. 570. 1998: National Renewable Energy Laboratory Golden, CO.
6. Abdoulmoumine, N., et al., *A review on biomass gasification syngas cleanup.* Applied Energy, 2015. **155**: p. 294-307.
7. Kiel, J., et al., *Primary measures to reduce tar formation in fluidised-bed biomass gasifiers.* ECN, ECN-C-04-014, 2004.
8. Devi, L., K.J. Ptasinski, and F.J.J.G. Janssen, *A review of the primary measures for tar elimination in biomass gasification processes.* Biomass and Bioenergy, 2003. **24**(2): p. 125-140.
9. Thunman, H., A. Larsson, and M. Hedenskog, *Commissioning of the GoBiGas 20MW Bio-methane Plant*, in *tcbiomass2015*. 2015: Chicago.
10. Pfeifer, C., R. Rauch, and H. Hofbauer, *In-Bed Catalytic Tar Reduction in a Dual Fluidized Bed Biomass Steam Gasifier.* Industrial & Engineering Chemistry Research, 2004. **43**(7): p. 1634-1640.
11. Lv, D., et al., *Effect of cellulose, lignin, alkali and alkaline earth metallic species on biomass pyrolysis and gasification.* Fuel Processing Technology, 2010. **91**(8): p. 903-909.
12. Fuentes-Cano, D., et al., *The influence of temperature and steam on the yields of tar and light hydrocarbon compounds during devolatilization of dried sewage sludge in a fluidized bed.* Fuel, 2013. **108**: p. 341-350.
13. de Andrés, J.M., A. Narros, and M.E. Rodríguez, *Behaviour of dolomite, olivine and alumina as primary catalysts in air-steam gasification of sewage sludge.* Fuel, 2011. **90**(2): p. 521-527.
14. Sutton, D., B. Kelleher, and J.R.H. Ross, *Review of literature on catalysts for biomass gasification.* Fuel Processing Technology, 2001. **73**(3): p. 155-173.
15. Speight, J.G., *Refining Chemistry*, in *The Chemistry and Technology of Petroleum*. 2006, Boca Raton: CRC Press.
16. Zimmermann, H. and R. Walzi, *Ethylene*, in *Encyclopedia of industrial chemistry*. 2012, Wiley-VCH Verlag GmbH & Co. KGaA.
17. Evans, R.J. and T.A. Milne, *Molecular characterization of the pyrolysis of biomass.* Energy & Fuels, 1987. **1**(2): p. 123-137.

18. Rostrup-Nielsen, J.R., *Catalytic steam reforming*, in *Catalysis*. 1984, Springer. p. 1-117.
19. Gómez-Barea, A. and B. Leckner, *Modeling of biomass gasification in fluidized bed.* Progress in Energy and Combustion Science, 2010. **36**(4): p. 444-509.
20. Trimm, D.L., *Coke formation and minimisation during steam reforming reactions.* Catalysis Today, 1997. **37**(3): p. 233-238.
21. Lind, F., et al., *Ilmenite and Nickel as Catalysts for Upgrading of Raw Gas Derived from Biomass Gasification.* Energy & Fuels, 2013. **27**(2): p. 997-1007.
22. Berguerand, N., et al., *Producer gas cleaning in a dual fluidized bed reformer—a comparative study of performance with ilmenite and a manganese oxide as catalysts.* Biomass Conversion and Biorefinery, 2012. **2**(3): p. 245-252.
23. Berguerand, N., et al., *Use of alkali-feldspar as bed material for upgrading a biomass-derived producer gas from a gasifier.* Chemical Engineering Journal, 2016. **295**(Supplement C): p. 80-91.
24. Zhang, J., et al., *Recent studies on chemical engineering fundamentals for fuel pyrolysis and gasification in dual fluidized bed.* Industrial & Engineering Chemistry Research, 2013. **52**(19): p. 6283-6302.
25. Rostrup-Nielsen, J.R., *Syngas in perspective.* Catalysis today, 2002. **71**(3): p. 243-247.
26. Salatino, P. and R. Solimene, *Mixing and segregation in fluidized bed thermochemical conversion of biomass.* Powder Technology, 2017. **316**: p. 29-40.
27. Moud, P.H., et al., *Effect of gas phase alkali species on tar reforming catalyst performance: Initial characterization and method development.* Fuel, 2015. **154**: p. 95-106.
28. Alstrup, I., J.R. Rostrup-Nielsen, and S. Røen, *High temperature hydrogen sulfide chemisorption on nickel catalysts.* Applied Catalysis, 1981. **1**(5): p. 303-314.
29. Rabou, L.P.L.M. and M.H.F. Overwijk, *The Alkmaar 4 MW bio-SNG demo project* in *3rd International Conference on Renewable Energy Gas Technology* 2016: Malmö, Sweden.
30. Kirnbauer, F., et al., *The positive effects of bed material coating on tar reduction in a dual fluidized bed gasifier.* Fuel, 2012. **95**: p. 553-562.
31. Wilk, V. and H. Hofbauer, *Analysis of optimization potential in commercial biomass gasification plants using process simulation.* Fuel Processing Technology, 2016. **141**(Part 1): p. 138-147.
32. Kuba, M., et al., *Influence of controlled handling of solid inorganic materials and design changes on the product gas quality in dual fluid bed gasification of woody biomass.* Applied Energy, 2018. **210**(Supplement C): p. 230-240.
33. Thunman, H., et al., *Advanced biofuel production via gasification – lessons learned from 200 man-years of research activity with Chalmers' research gasifier and the GoBiGas demonstration plant.* Energy Science & Engineering, 2018. **6**(1): p. 6-34.
34. Wilk, V., J.C. Schmid, and H. Hofbauer, *Influence of fuel feeding positions on gasification in dual fluidized bed gasifiers.* Biomass and Bioenergy, 2013. **54**(0).
35. Benedikt, F., et al., *Advanced dual fluidized bed steam gasification of wood and lignite with calcite as bed material.* Korean Journal of Chemical Engineering, 2017. **34**(9): p. 2548-2558.

36. Zhang, Y., B. Jin, and W. Zhong, *Experimental investigation on mixing and segregation behavior of biomass particle in fluidized bed.* Chemical Engineering and Processing: Process Intensification, 2009. **48**(3): p. 745-754.

37. Kunii, D. and O. Levenspiel, *Fluidization Engineering (Second Edition)*. 1991, Boston: Butterworth-Heinemann. 61-94.

38. Larsson, A., et al., *Evaluation of Performance of Industrial-Scale Dual Fluidized Bed Gasifiers Using the Chalmers 2-4-MWth Gasifier.* Energy & Fuels, 2013. **27**(11).

39. Herguido, J., J. Corella, and J. Gonzalez-Saiz, *Steam gasification of lignocellulosic residues in a fluidized bed at a small pilot scale. Effect of the type of feedstock.* Industrial & Engineering Chemistry Research, 1992. **31**(5): p. 1274-1282.

40. Zhang, Y., et al., *Tar destruction and coke formation during rapid pyrolysis and gasification of biomass in a drop-tube furnace.* Fuel, 2010. **89**(2): p. 302-309.

41. Lundberg, L., et al., *Determination of Kinetic Parameters for the Gasification of Biomass Char Using a Bubbling Fluidized Bed Reactor*, in *22nd International Conference on Fluidized Bed Conversion*. 2015: Turku, Finland.

42. Ming, Q., et al., *Steam reforming of hydrocarbon fuels.* Catalysis Today, 2002. **77**(1-2): p. 51-64.

43. Marinkovic, J., *Choice of bed material: a critical parameter in the optimization of dual fluidized bed systems*, in *Energy and Environment*. 2016, Chalmers University of Technology.

44. Virginie, M., et al., *Effect of Fe-olivine on the tar content during biomass gasification in a dual fluidized bed.* Applied Catalysis B: Environmental, 2012. **121-122**(0): p. 214-222.

45. Pfeifer, C., S. Koppatz, and H. Hofbauer, *Steam gasification of various feedstocks at a dual fluidised bed gasifier: Impacts of operation conditions and bed materials.* Biomass Conversion and Biorefinery, 2011. **1**(1): p. 39-53.

46. Cuadrat, A., et al., *Behavior of ilmenite as oxygen carrier in chemical-looping combustion.* Fuel Processing Technology, 2012. **94**(1): p. 101-112.

47. Mendiara, T., et al., *Biomass combustion in a CLC system using an iron ore as an oxygen carrier.* International Journal of Greenhouse Gas Control, 2013. **19**(0): p. 322-330.

48. Keller, M., et al., *Gasification inhibition in chemical-looping combustion with solid fuels.* Combustion and Flame, 2011. **158**(3): p. 393-400.

49. Lind, F., et al., *Manganese oxide as catalyst for tar cleaning of biomass-derived gas.* Biomass Conversion and Biorefinery, 2012. **2**(2): p. 133-140.

50. Larsson, A., et al., *Using Ilmenite To Reduce the Tar Yield in a Dual Fluidized Bed Gasification System.* Energy & Fuels, 2014. **28**(4): p. 2632-2644.

51. Heyne, S. and S. Harvey, *Impact of choice of CO2 separation technology on thermo-economic performance of Bio-SNG production processes.* International Journal of Energy Research, 2014. **38**(3): p. 299-318.

52. Vitasari, C.R., M. Jurascik, and K.J. Ptasinski, *Exergy analysis of biomass-to-synthetic natural gas (SNG) process via indirect gasification of various biomass feedstock.* Energy, 2011. **36**(6): p. 3825-3837.

53. Adánez, J., et al., *Chemical looping combustion of solid fuels.* Progress in Energy and Combustion Science, 2018. **65**: p. 6-66.
54. Abad, A., et al., *Mapping of the range of operational conditions for Cu-, Fe-, and Ni-based oxygen carriers in chemical-looping combustion.* Chemical Engineering Science, 2007. **62**(1-2): p. 533-549.
55. Elliott, D.C., *Relation of Reaction Time and Temperature to Chemical Composition of Pyrolysis Oils*, in *Pyrolysis Oils from Biomass*. 1988, American Chemical Society. p. 55-65.
56. Patwardhan, P.R., R.C. Brown, and B.H. Shanks, *Understanding the Fast Pyrolysis of Lignin.* ChemSusChem, 2011. **4**(11): p. 1629-1636.
57. Norinaga, K., et al., *Detailed chemical kinetic modelling of vapour-phase cracking of multi-component molecular mixtures derived from the fast pyrolysis of cellulose.* Fuel, 2013. **103**: p. 141-150.
58. Cypres, R., *Aromatic hydrocarbons formation during coal pyrolysis.* Fuel Processing Technology, 1987. **15**: p. 1-15.
59. Lovell, A.B., K. Brezinsky, and I. Glassman, *The gas phase pyrolysis of phenol.* International Journal of Chemical Kinetics, 1989. **21**(7): p. 547-560.
60. Jess, A., *Mechanisms and kinetics of thermal reactions of aromatic hydrocarbons from pyrolysis of solid fuels.* Fuel, 1996. **75**(12): p. 1441-1448.
61. Dufour, A., et al., *Evolution of Aromatic Tar Composition in Relation to Methane and Ethylene from Biomass Pyrolysis-Gasification.* Energy & Fuels, 2011. **25**(9): p. 4182-4189.
62. Morf, P., P. Hasler, and T. Nussbaumer, *Mechanisms and kinetics of homogeneous secondary reactions of tar from continuous pyrolysis of wood chips.* Fuel, 2002. **81**(7): p. 843-853.
63. Frenklach, M. and H. Wang, *Detailed Mechanism and Modeling of Soot Particle Formation*, in *Soot Formation in Combustion: Mechanisms and Models*, H. Bockhorn, Editor. 1994, Springer Berlin Heidelberg: Berlin, Heidelberg. p. 165-192.
64. Sharma, R.K. and M.R. Hajaligol, *Effect of pyrolysis conditions on the formation of polycyclic aromatic hydrocarbons (PAHs) from polyphenolic compounds.* Journal of Analytical and Applied Pyrolysis, 2003. **66**(1): p. 123-144.
65. Richter, H. and J.B. Howard, *Formation of polycyclic aromatic hydrocarbons and their growth to soot—a review of chemical reaction pathways.* Progress in Energy and Combustion Science, 2000. **26**(4): p. 565-608.
66. Norinaga, K., et al., *Numerical simulation of thermal conversion of aromatic hydrocarbons in the presence of hydrogen and steam using a detailed chemical kinetic model.* Chemical Engineering Journal, 2011. **178**: p. 282-290.
67. Marinkovic, J., et al., *Characteristics of olivine as a bed material in an indirect biomass gasifier.* Chemical Engineering Journal, 2015. **279**: p. 555-566.
68. Marinkovic, J., et al., *Impact of biomass ash – bauxite bed interactions on an indirect biomass gasifier.* (Recently submitted to Energy & Fuels), 2016.
69. Berguerand, N. and T. Berdugo Vilches, *Alkali-Feldspar as a Catalyst for Biomass Gasification in a 2-MW Indirect Gasifier.* Energy & Fuels, 2017. **31**(2): p. 1583-1592.
70. Vassilev, S.V., et al., *An overview of the chemical composition of biomass.* Fuel, 2010. **89**(5): p. 913-933.

71. Kirnbauer, F. and H. Hofbauer, *Investigations on Bed Material Changes in a Dual Fluidized Bed Steam Gasification Plant in Güssing, Austria.* Energy & Fuels, 2011. **25**(8): p. 3793-3798.

72. Knutsson, P., et al., *Role of potassium in the enhancement of the catalytic activity of calcium oxide towards tar reduction.* Applied Catalysis B: Environmental, 2018. **229**: p. 88-95.

73. Marinkovic, J., et al., *Impact of Biomass Ash-Bauxite Bed Interactions on an Indirect Biomass Gasifier.* Energy & Fuels, 2016. **30**(5): p. 4044-4052.

74. Boström, D., et al., *Ash Transformation Chemistry during Combustion of Biomass.* Energy & Fuels, 2012. **26**(1): p. 85-93.

75. Zevenhoven, M., P. Yrjas, and M. Hupa, *Ash-Forming Matter and Ash-Related Problems*, in *Handbook of Combustion*. 2010, Wiley-VCH Verlag GmbH & Co. KGaA.

76. Frandsen, F.J., *Ash formation, deposition and corrosion when utilizing straw for heat and power production*, in *Department of Chemical and Biochemical Engineering*. 2011, Technical University of Denmark.

77. Novaković, A., et al., *Release of Potassium from the Systems K-Ca-Si and K-Ca-P.* Energy & Fuels, 2009. **23**(7): p. 3423-3428.

78. Öhman, M., L. Pommer, and A. Nordin, *Bed Agglomeration Characteristics and Mechanisms during Gasification and Combustion of Biomass Fuels.* Energy & Fuels, 2005. **19**(4): p. 1742-1748.

79. Kuba, M., et al., *Mechanism of Layer Formation on Olivine Bed Particles in Industrial-Scale Dual Fluid Bed Gasification of Wood.* Energy & Fuels, 2016. **30**(9): p. 7410-7418.

80. He, H., N. Skoglund, and M. Öhman, *Time-Dependent Layer Formation on K-Feldspar Bed Particles during Fluidized Bed Combustion of Woody Fuels.* Energy & Fuels, 2017. **31**(11): p. 12848-12856.

81. Kirnbauer, F., et al., *Behavior of inorganic matter in a dual fluidized steam gasification plant.* Energy & Fuels, 2013. **27**(6): p. 3316-3331.

82. Kuba, M., et al., *Deposit build-up and ash behavior in dual fluid bed steam gasification of logging residues in an industrial power plant.* Fuel Processing Technology, 2015. **139**: p. 33-41.

83. Pissot, S., et al., *Effect of ash circulation on the performance of a dual fluidized bed gasification system.* Biomass and Bioenergy, 2018. **115**: p. 45-55.

84. Veraa, M.J. and A.T. Bell, *Effect of alkali metal catalysts on gasification of coal char.* Fuel, 1978. **57**(4): p. 194-200.

85. Wigmans, T., R. Elfring, and J.A. Moulijn, *On the mechanism of the potassium carbonate catalysed gasification of activated carbon: the influence of the catalyst concentration on the reactivity and selectivity at low steam pressures.* Carbon, 1983. **21**(1): p. 1-12.

86. Liu, Z.-l. and H.-h. Zhu, *Steam gasification of coal char using alkali and alkaline-earth metal catalysts.* Fuel, 1986. **65**(10): p. 1334-1338.

87. Johansson, L., et al., *Particle emissions from biomass combustion in small combustors.* Biomass and bioenergy, 2003. **25**(4): p. 435-446.

88. Hüttinger, K.J. and R. Minges, *The influence of the catalyst precursor anion in catalysis of water vapour gasification of carbon by potassium: 2. Catalytic activity by activation and deactivation reactions.* Fuel, 1986. **65**(8): p. 1122-1128.

89. Adler, J. and K.J. Hüttinger, *Mixtures of potassium sulphate and iron sulphate as catalysts for water vapour gasification of carbon. 1. Kinetic studies.* Fuel, 1984. **63**(10): p. 1393-1396.
90. Keller, M., H. Leion, and T. Mattisson, *Mechanisms of Solid Fuel Conversion by Chemical-Looping Combustion (CLC) using Manganese Ore: Catalytic Gasification by Potassium Compounds.* Energy Technology, 2013. **1**(4): p. 273-282.
91. Kuba, M., et al., *Influence of bed material coatings on the water-gas-shift reaction and steam reforming of toluene as tar model compound of biomass gasification.* Biomass and Bioenergy, 2016. **89**: p. 40-49.
92. Kuba, M., F. Kirnbauer, and H. Hofbauer, *Influence of coated olivine on the conversion of intermediate products from decomposition of biomass tars during gasification.* Biomass Conversion and Biorefinery, 2017. **7**(1): p. 11-21.
93. Hayashi, J.-I., et al., *Roles of inherent metallic species in secondary reactions of tar and char during rapid pyrolysis of brown coals in a drop-tube reactor.* Fuel, 2002. **81**(15): p. 1977-1987.
94. Umeki, K., et al., *Reduction of Tar and Soot Formation from Entrained-Flow Gasification of Woody Biomass by Alkali Impregnation.* Energy & Fuels, 2017. **31**(5): p. 5104-5110.
95. Hindiyarti, L., et al., *Influence of potassium chloride on moist CO oxidation under reducing conditions: Experimental and kinetic modeling study.* Fuel, 2006. **85**(7): p. 978-988.
96. Jiang, L., et al., *Catalytic behaviors of alkali metal salt involved in homogeneous volatile and heterogeneous char reforming in steam gasification of cellulose.* Energy Conversion and Management, 2018. **158**: p. 147-155.
97. Debiagi, P.E.A., et al., *Detailed kinetic mechanism of gas-phase reactions of volatiles released from biomass pyrolysis.* Biomass and Bioenergy, 2016. **93**: p. 60-71.
98. Huyghe, J., *The role of alkali and earth alkaline metals as intrinsic catalysts in the fast pyrolysis of biomass constituents*, in *Faculty of Bioscience Engineering*. 2014, University of Gent.
99. Corella, J., et al., *Biomass Gasification in Fluidized Bed: Where To Locate the Dolomite To Improve Gasification?* Energy & Fuels, 1999. **13**(6): p. 1122-1127.
100. Israelsson, M., M. Seemann, and H. Thunman, *Assessment of the Solid-Phase Adsorption Method for Sampling Biomass-Derived Tar in Industrial Environments.* Energy & Fuels, 2013. **27**(12): p. 7569-7578.
101. Brage, C., et al., *Use of amino phase adsorbent for biomass tar sampling and separation.* Fuel, 1997. **76**(2): p. 137-142.
102. Israelsson, M., A. Larsson, and H. Thunman, *Online Measurement of Elemental Yields, Oxygen Transport, Condensable Compounds, and Heating Values in Gasification Systems.* Energy & Fuels, 2014. **28**(9): p. 5892-5901.
103. Rapagnà, S., et al., *Steam-gasification of biomass in a fluidised-bed of olivine particles.* Biomass and Bioenergy, 2000. **19**(3): p. 187-197.
104. Neves, D.d.S.F.d., *Evaluation of thermochemical biomass conversion in fluidized bed*, in *Department of Environment and Planning, and Center of Environmental and Marine Studies*. 2013, Universidade de Aveiro.

105. Israelsson, M., T. Berdugo Vilches, and H. Thunman, *Conversion of Condensable Hydrocarbons in a Dual Fluidized Bed Biomass Gasifier.* Energy & Fuels, 2015.
106. Leion, H., T. Mattisson, and A. Lyngfelt, *Solid fuels in chemical-looping combustion.* International Journal of Greenhouse Gas Control, 2008. **2**(2): p. 180-193.
107. Pfeifer, C., et al., *Next generation biomass gasifier*, in *Proc. 19th European Biomass Conference and Exhibition*. 2011: Berlin, Germany.